OCEAN DRILLING PROGRAM

LEG 184 SCIENTIFIC PROSPECTUS

SOUTH CHINA SEA

Dr. Warren L. Prell
Co-Chief Scientist
Department of Geological Sciences
Brown University
Box 1846
Providence, RI 02912
U.S.A.

Dr. Pinxian Wang
Co-Chief Scientist
Department of Marine Geology
Tongji University
Shanghai 200092
People's Republic of China

Dr. Peter Blum
Staff Scientist
Ocean Drilling Program
Texas A&M University Research Park
1000 Discovery Drive
College Station, TX 77845-9547
U.S.A.

Jack Baldauf
Deputy Director
of Science Operations
ODP/TAMU

Peter Blum
Leg Project Manager
Science Services
ODP/TAMU

September 1998

Scientific Prospectus No. 84
First Printing 1998
Distribution

Electronic copies of this publication may be obtained from the ODP Publications homepage on the World Wide Web at: http://www-odp.tamu.edu/publications

D I S C L A I M E R

This publication was prepared by the Ocean Drilling Program, Texas A&M University, as an account of work performed under the international Ocean Drilling Program, which is managed by Joint Oceanographic Institutions, Inc., under contract with the National Science Foundation. Funding for the program is provided by the following agencies:

Australia/Canada/Chinese Taipei/Korea Consortium for Ocean Drilling
Deutsche Forschungsgemeinschaft (Federal Republic of Germany)
Institut Français de Recherche pour l'Exploitation de la Mer (France)
Ocean Research Institute of the University of Tokyo (Japan)
National Science Foundation (United States)
Natural Environment Research Council (United Kingdom)
European Science Foundation Consortium for the Ocean Drilling Program (Belgium, Denmark, Finland, Iceland, Italy, The Netherlands, Norway, Portugal, Spain, Sweden, and Switzerland)
People's Republic of China

Any opinions, findings, and conclusions or recommendations expressed in this publication are those of the author(s) and do not necessarily reflect the views of the National Science Foundation, the participating agencies, Joint Oceanographic Institutions, Inc., Texas A&M University, or Texas A&M Research Foundation.

This Scientific Prospectus is based on precruise JOIDES panel discussions and scientific input from the designated Co-chief Scientists on behalf of the drilling proponents. The operational plans within reflect JOIDES Planning Committee and thematic panel priorities. During the course of the cruise, actual site operations may indicate to the Co-chief Scientists and the Operations Manager that it would be scientifically or operationally advantageous to amend the plan detailed in this prospectus. It should be understood that any proposed changes to the plan presented here are contingent upon approval of the Director of the Ocean Drilling Program in consultation with the Science and Operations Committees (successors to the Planning Committee) and the Pollution Prevention and Safety Panel (PPSP).

Technical Editor: Karen K. Graber

ABSTRACT

During Leg 184 we will core hemipelagic sediments in the South China Sea (SCS) to determine the evolution and variability of the East Asian monsoon during the late Cenozoic. Of the six primary proposed drill sites, five are located on the northern continental slope of the SCS in water depths ranging from 1265 m to 3190 m. In the southern SCS, one site will be located on the southern margin in 2830 m water depth.

The major goals of Leg 184 are to improve our knowledge about the variability of monsoonal climates, including millennial to possibly centennial variability from high-sedimentation rate records (SCS-1), orbital-scale variability from records at all SCS sites, and tectonic-scale variability from late Cenozoic sections (Sites SCS-4 and 5). The records from the SCS will be used to establish the links between the East Asian and Indian monsoons and to evaluate mechanisms of internal (climate system feedbacks) and external (orbital and tectonic) climate forcing. We seek to test a suite of hypotheses that link uplift of the Himalayan and Tibetan Plateau complex (HTC) to both the intensification of the Asian monsoon and late Cenozoic global cooling. The proposed drilling program in the SCS will enable comparison of the Chinese terrestrial record with the marine records of monsoonal climates and hence provide an additional regional constraint on the scenarios for monsoon evolution.

Leg 184 has a number of related major scientific objectives:

1. obtain continuous sequences of hemipelagic sediments that record the East Asian climate history during the late Cenozoic;
2. establish records of monsoonal proxies for the SCS, including the variability of sediment properties, the rates of sediment accumulation, and the chemical, isotopic, and species variability of flora and fauna;
3. establish stratigraphic ties between the SCS marine record and the terrestrial records of China;
4. establish the relationship of East Asian monsoon variability with orbital forcing, glacial forcing, and internal feedbacks within the climate system;

5. compare the evolution of the East Asian monsoon in the SCS with the Indian monsoon in the Arabian Sea to identify common causality;
6. test several proposed scenarios for the relationship between the Tibetan Plateau uplift, monsoon evolution, and global cooling; and
7. improve our understanding of seasonality in the low-latitude SCS and how it relates to the stability of the Western Pacific Warm Pool and the strength and evolution of the winter monsoon.

INTRODUCTION

The Asian monsoon is one of the major components of the global climate system and its evolution plays a significant role in our understanding of global climates (Fig. 1) (Hastenrath, 1991; Hastenrath and Greischar, 1993; Webster, 1987; Webster, 1994; Webster et al., 1998). The Asian summer and winter monsoons dominate the seasonal winds, precipitation and runoff patterns, and the character of land vegetation over southern and eastern Asia. The winter monsoon is characterized by high pressure over northern Asia, northeast winds across the South China Sea (SCS) (which intensify during cold surges), and enhanced precipitation in the Austral-Asian equatorial zone (Fig. 1A, 1C). The summer monsoon circulation is characterized by low pressure over Tibet, strong southwesterly winds, upwelling in the Arabian Sea, and high precipitation over southern and eastern Asia (Fig. 1B, 1D). The SCS is ideally located to record the paleoceanographic responses to both winter and summer monsoons (Figs. 1, 2). Evolution of the Asian monsoon system is thought to reflect at least four types of large-scale climate forcing or boundary conditions: (1) the tectonic development of the Himalayan-Tibetan orography, (2) changes in the atmospheric CO_2 concentration, (3) changes in the Earth's orbital parameters and the resulting variations in seasonal solar radiation, and (4) changes in the extent of glacial climates. These factors act to amplify or dampen the seasonal development of land-sea heating and pressure gradients, latent heat transport, and moisture convergence over the Asian continent.

Mountain-Plateau Uplift Forcing

The effects of tectonically induced orographic changes on the monsoon system provide an explanation for its initiation, intensification, and long-term (10^6 yr) evolution (see the papers and references in Ruddiman, 1997). Prior to the collision of India with Asia, the Himalayas and Tibet did not exist in their present state, and the Asian continent was not as large. The smaller size and lower elevations of the pre-collision continent might be expected to support a lower land-sea heating contrast because of the important role of sensible heating over the plateau and the condensational heating over and on the flanks of the Tibetan Plateau. In general, the modern monsoon circulation would not exist if the Himalayas and Tibet were not at their present location and elevation. For the summer monsoon, the thermal effects, both sensible and latent heating, of the Himalayan and Tibetan Plateau complex (HTC) are the major impact of the orographic forcing. During the winter monsoon, the thermal effects of the HTC are thought to be small, but the mechanical effects, such as blocking and directing low-level winds and the development of cold surges, are the major impacts of the orography (Murakami, 1987). The SCS should provide an especially good record of the winter monsoon evolution and its relationship to the evolving orography of Asia.

CO_2 Forcing

A variety of observations have suggested that CO_2 levels were higher during the Tertiary and may have been equivalent to double the present CO_2 levels at ~20 Ma (see Kump and Arthur, 1997 and other papers in Ruddiman, 1997). Higher CO_2 levels might be expected to strengthen the summer monsoon through increased land-sea contrasts and more active hydrologic budgets but might also weaken the winter monsoon through warmer continents. Lowered CO_2 levels are thought to have caused global changes in vegetation from C3 to C4 ~7 Ma (see Fig. 3), which also has implications for monsoonal processes related to soil moisture, albedo, and carbon cycling (Cerling, 1997). Hence, the strength of winter monsoons in the SCS may covary with both increased orography and decreased CO_2.

Orbital Forcing

Changes in the Earth's orbit result in redistribution of solar energy over the surface of the Earth. For example, during high eccentricity intervals the precessional-driven summer season radiation budget over the Tibetan Plateau can vary as much as $\pm$12.5% (relative to modern values of 450 W/m^2). Numerous studies of Indian Ocean and western Pacific sediments reveal that a number of monsoon indicators (upwelling fauna, productivity, dust particle size, and vegetation types) vary coherently with orbital periodicities (Prell, 1984a, 1984b; Clemens et al., 1991; Morley and Heusser, 1997). However, the monsoonal indices are not always in direct proportion or in phase with the apparent solar forcing. The phase of monsoonal responses in the SCS should provide additional constraints on the relative importance of orbital forcing and internal feedbacks on monsoonal variability.

Glacial Climate Forcing

The extent of glacial-age surface boundary conditions also affects the monsoon system (Prell and Kutzbach, 1987, 1992). Numerous studies have shown that more extensive glacial climates tend to weaken the summer monsoon (Clemens et al., 1996), although glacial intervals do contain strong monsoons (Clemens and Prell, 1991). These responses result from the lower sea surface temperature, lower sea level, higher albedo of the land surface, and the extent and elevation of large ice masses (CLIMAP, 1976, 1981). However, more extensive glacial climates may strengthen the winter monsoon, especially as recorded in the SCS.

Given these potential "causal" factors, our goal is to understand their relative importance in the initiation, evolution, and variability of the Asian monsoon system. Hence, one of the long-term goals of Leg 184 is to decipher how the tectonic development of Asia, the Asian monsoon circulation, and global climate have co-evolved during the Neogene.

Despite the importance and interconnections of the two monsoonal subsystems (East Asian and Indian), previous marine-based studies of past monsoonal variations have concentrated on the Indian monsoon (Prell, Niitsuma, et al., 1991; Prell et al., 1992 and references within). The East Asian paleomonsoon studies have been restricted mainly to land-based work, with monsoon information commonly being obtained from the Chinese loess. Less attention has been paid to the marine aspects of the East Asian monsoon until recently. Extensive hydrocarbon exploration in China and its surrounding offshore areas has accumulated extensive geological data that are rich in Cenozoic paleomonsoon information. Together with recent progress in Quaternary science for East Asia and the western Pacific (e.g., Liu and Ding, 1993; Wang, 1990), the data have led to the development of a four-stage model of East Asian monsoon evolution: a premonsoon stage (Paleocene and early Eocene), a transitional stage (late Eocene to Oligocene), a monsoon Stage I (Miocene and Pliocene), and a monsoon Stage II (late Pliocene [2.4 Ma] to present) (Table 1; Wang, 1997).

Palynologic, paleobotanic, and lithologic data (Fig. 4C) indicate that the climate pattern in China underwent a profound reorganization around the beginning of the Neogene (Wang, 1990; Sun and Wang, pers. comm., 1998). The Paleocene in China inherited the Late Cretaceous environmental pattern ("Pre-monsoon Stage"), with a broad arid zone traversing the whole country from west to east (Fig. 4A). The middle-late Eocene and Oligocene climate in China ("Transitional Stage") was characterized by variable, weak summer monsoons that brought moisture to the otherwise dry areas, which created the most favorable conditions for nonmarine oil accumulation in China. During the Miocene, the arid zone retreated to northwest China, and eastern China became more humid (Fig. 4B; "Monsoon Stage I") as the southeast summer monsoon strengthened and brought moisture

Table 1. Evolution stages of the East Asian monsoon in the Cenozoic, based on land studies from China.

Stage	Time interval	Monsoon	Paleogeography
Premonsoon	Paleocene to early Eocene	Absent or insignificant	Smaller Asia without Tibetan Plateau
Transitional	late Eocene to Oligocene	Weak	India joined with Asia
Monsoon I	Miocene to Pliocene	Summer monsoon developed	Plateau uplift started
Monsoon II	late Pliocene to Pleistocene	Summer and winter monsoon developed	Intensive plateau uplift

from the sea. This general regime has existed from the Miocene to the Holocene. The intensification of the winter monsoon in eastern Asia is thought to occur much later, and to have marked the beginning of deposition of the Chinese loess deposits at about 2.4 Ma ("Monsoon Stage II"; Liu and Ding, 1982). The loess deposits are a joint product of winter and summer monsoons and thus imply that both systems are active. However, some recent studies suggest that the eolian component of the loess red-clay sequence may have began as early as 7 Ma (Ding et al., 1998), which would have implications for the tectonic vs. glacial initiation and intensification of the winter monsoon.

Among the continents of the world, Asia has been subjected to the most significant Cenozoic deformation. The Cretaceous-Paleocene topography of China was generally tilted to the west, with the coastal areas of the Tethys in the west and relatively high land and endorheic basins in the east. This paleogeographic pattern lasted until the late Eocene when India collided with Asia, thereby bringing the maritime conditions in western China to an end. The uplift of the Tibetan Plateau may have started about 21-20 Ma (Copeland et al., 1987; Harrison et al., 1991) and was accompanied by a general subsidence of East China. Other studies (Molnar et al., 1993) suggest that the Tibetan Plateau was uplifted rapidly about 10 Ma and has been subsiding since the middle Miocene. These tectonic changes led to a reversal of the topographic trend in China from west tilting to east tilting, with the west-east gradient in altitude increasing continuously since then. In addition, the early Miocene was also the time of formation for many of the western Pacific marginal seas. The radical changes that occurred in the topography of Asia during the Cenozoic must have had a profound impact on climate, including the onset or strengthening of the monsoon circulation in East Asia. The further development of east-sloping topography and monsoon precipitation has brought about the large river systems, which discharge enormous amounts of sediments into the newly formed marginal seas along the East Asian coast and build extensive coastal plains and continental shelves.

Because the Indian and East Asian monsoons share the same tectonic factor in their evolution, we would expect to find synchronous evolutionary stages. Deep Sea Drilling Project (DSDP) and Ocean Drilling Program (ODP) core studies have revealed the onset of clastic deep-sea fan sedimentation at about 20 Ma, which may be related to monsoon runoff (Cochran, 1990). Both marine and terrestrial data indicate a major intensification of the Indian monsoon around 8 Ma (Fig. 3) (Prell, et al., 1992 and references within; Prell and Kutzbach, 1992). If the East Asian monsoon record in the SCS supports this timing, it will be a strong argument in support of tectonic forcing as a cause for intensification of both Asian monsoons.

The accelerating uplift of the Tibetan Plateau is thought to be responsible not only for the intensification of the Asian monsoon, but also for late Cenozoic global cooling (e.g., Ruddiman and Kutzbach, 1989). Raymo et al. (1988) proposed that long-term increased chemical erosion in rapidly uplifted areas could reduce atmospheric CO_2 (Raymo, 1994) and thereby cool the planet and enable widespread glaciation. If this is the case, the evolution of Asian monsoon and global cooling should be correlated with each other. The proposed drilling in the SCS will test for causal relationships between the three major environmental features in the late Cenozoic (1) global cooling, (2) enhanced chemical and physical weathering, and (3) onset/intensification of the Asian monsoon.

GEOLOGIC FRAMEWORK FOR THE SOUTH CHINA SEA

Tectonic Setting

The opening of the SCS was genetically related to the deformation of Asia. The rhomboid-shaped Central Basin is the major deep-water oceanic crust feature of the SCS (Fig. 5A). Judging from the magnetic anomalies in the SCS Central Basin, seafloor spreading lasted from 32 Ma (magnetic Anomaly 11) to 16 Ma (Anomaly 5c), with a southward ridge jump at ~27 Ma (Anomaly 7/6b) (Briais et al., 1993). The opening of the SCS basin is thought to be linked with the Red River fault zone, which has at least 500 to 600 km of left-lateral displacement during the Oligocene and Miocene (Schärer et al., 1990; Briais et al., 1993). The slopes of the SCS contain numerous coral reef terrain systems that migrated during the SCS opening: the Nansha Terrain (Reed Bank and Dangerous Ground), the Xisha-Zhongsha Terrain (Macclesfield Bank and Paracel Island) and others (Jin, 1992).

The northern continental margin of the SCS has been extensively studied as part of oil exploration and geophysical studies to determine the amount of crustal extension during formation of the SCS (e.g., Hayes et al., 1995). The sedimentary basins of the northern shelf show a typical double-layer structure, with a lower section characterized by half grabens formed during Paleogene rifting and an upper section characterized by a wider distribution of deposits formed during the broad subsidence in the Neogene (Fig. 5B; Ru et al., 1994).

Sedimentology and Stratigraphy

Modern sediments in the SCS consist mainly of terrigenous material, biogenic carbonate and opal, and a small portion of volcanic material. Clastic sediment is mainly discharged into the SCS from the Mekong River, Red River, and Pearl River. However, during the past glacial intervals, the paleo-Sunda River system provided a great amount of sediment into the SCS. Recent sediment trap studies in the northern SCS have shown that the highest particle-flux rates are correlated with high wind speed during the winter monsoon and, hence, the suspended matter from the East China Sea and the Pacific may exceed the amount of river input into the northern SCS (Jennerjahn et al., 1992). With the high terrigenous input and the location of the modern carbonate compensation depth (CCD) at 3500 m, the extensive continental slopes of the SCS are dominated by hemipelagic sediments; whereas, the deep-sea basin is covered by abyssal clay, and biogenic carbonates are found around coral reef islands. Two types of carbonate cycles are found in the late Quaternary SCS: the "Atlantic" type (above the lysocline), where the controlling factor is dilution by terrigenous clasts, and the "Pacific" type (below the lysocline), where deep-sea dissolution is the controlling factor (Wang et al., 1986; Bian et al., 1992; Thunell et al., 1992; Zheng et al., 1993; Miao et al., 1994; Wang et al., 1995b).

The shelf basins on the SCS contain thousands of meters of Cenozoic deposits that have been drilled by petroleum companies. The basins have nonmarine sequences underlying marine sediments that were deposited during the Miocene or late Oligocene (Fig. 6). Reworked Paleocene and Eocene marine microfossils were present in Neogene deposits from the northern shelf, and Paleocene deltaic and Eocene marine sediments were found in the southern part of the SCS (Fig. 6) such as the Liyue Bank (Reed Bank) Basin, where carbonate deposition started from the middle Oligocene (ASCOPE, 1981; Jin, 1989). Among the basins in the northern SCS, the Pearl River Mouth Basin is the most studied. Over 150 wells have been drilled there and a detailed stratigraphy established for the marine sequence from the uppermost Oligocene to Pleistocene on the basis of various groups of planktonic microfossils (Huang, 1997). Of particular interest are the boreholes drilled on the continental slope in water depths over 500 m, such as Well BY 7-1-1, where the marine sequence ranges from NP23/24 to NN20 (see fig. 3 in Huang, 1997). On the basis of recent publications (Jiang et al., 1994; Wu, 1994; Huang, 1997), the Cenozoic stratigraphy of the Pearl River Mouth Basin is summarized in Figure 6. Noticeable is the presence of nonmarine intercalations in the northern part of the basin, thinning out and decreasing in proportion southward toward the deeper part of the slope. Major depositional hiatuses have been observed at least in the lower part of the lower Miocene, near the end of the middle Miocene, and around the Plio-Pleistocene boundary (L. Huang, pers. comm., 1998).

Late Quaternary Paleoceanography

During the last glacial maximum (LGM), sea-level lowering caused remarkable alteration in the configuration and area of the western Pacific marginal seas. The three major shelf areas that emerged during the LGM (East China Sea Shelf, Sunda Shelf or the Great Asian Bank [Fig. 7A], and Sahul Shelf or the Great Australian Bank) amount to 3,900,000 km^2, which is comparable in size to the Indian subcontinent. The SCS lost half of its area (>52%) as a result of shelf exposure, which changed its configuration into a semi-isolated basin (Wang et al., 1997). Moreover, the most extensive shelf area of the SCS is located in the modern Western Pacific Warm Pool bounded by the 28°C surface isotherm. The reduction in size must have profoundly influenced the thermodynamic role played by the Global Warm Pool.

The central portion of the SCS experienced a considerable decline in the sea-surface temperature (SST) during the LGM. The winter monsoon strengthened, the polar front shifted southward, and the Kuroshio Current migrated eastward. All of these changes caused a drastic decrease in the winter SST in the Western Pacific marginal seas in general and in the SCS particularly (Wang and Wang, 1990; Miao et al., 1994; Wang et al., 1995b). Together with the negligible changes in the summer SST, the decrease in winter SST resulted in a much more intensive seasonality during the LGM (Fig. 7B; Wang, in press). Among the important consequences of the glacial changes of the SCS is the intensified aridity in China. The SCS is the main source of water vapor for precipitation in East China (Chen et al., 1991). The above-described shelf emergence and SST decline must have led to a reduction in evaporation and vapor supply from the sea to the land. A very preliminary estimate shows that the reduction in evaporation from the SCS during the LGM could correspond to 1/8 to 1/4 of the annual precipitation in all of China (Wang et al., 1997). The glacial reduction in vapor supply from the sea at least partially explains the intensification of aridity in the China hinterland as evidenced, for example, by the extensive distribution of loess deposits. Moreover, the glacial increase of seasonality in the marginal seas may offer an alternate approach to the tropical paleoclimate enigma in the Pacific, that is, the discrepancy between marine and terrestrial indicators of paleotemperature during the LGM (Stuijts et al., 1988; Andersen and Webb, 1994).

The late Quaternary studies have demonstrated the great potential of the SCS's hemipelagic sediments to provide high-resolution paleoenvironment records. A core from the northern SCS (SONNE 17940) reveals a highly detailed transition from glacial to Holocene conditions (Wang et al., in press). On the basis of low fluvial clay content (50%-60%) and high modal grain size (10-25 μm) during the LGM and stage 3 and the transition to high clay content (>70%) and low modal grain size (<6.3 μm) in the Holocene (Fig. 8), a strong winter monsoon and weak summer monsoon precipitation are inferred for the glacial regime and a strong summer monsoon and weakened winter monsoon are inferred for the Holocene regime. The $\delta^{18}O$ data from the mixed layer planktonic foraminifer *Globigerinoides ruber* reveal numerous short-term light $\delta^{18}O$ events superimposed on the main pattern of glacial-postglacial change (Fig. 8). These events are interpreted to reflect increases in summer monsoon intensity, i.e., reduced sea-surface salinity together with increases of fluvial clay and decreases in modal grain size. The increases in summer monsoon intensity can be correlated with Dansgaard-Oeschger events 1-10 in the GISP2 ice core (Fig. 8). Also observed in this SCS core are four periods of relatively heavy $\delta^{18}O$ associated with low fluvial clay content and high grain size, i.e., reduced summer monsoon precipitation and increased winter monsoon wind, which correlate to the Heinrich events 1-4 (Fig. 8). The early Holocene/Pre Boreal (EHPB) summer monsoon maximum revealed by a broad $\delta^{18}O$ minimum and fluvial clay maximum has also been reported from the Arabian Sea (Prell, 1984b; Sorocko, et al., 1993). The 8.2k cooling event recorded in the GISP2 ice core appears to coincide with a large increase in $\delta^{18}O$ and hence decrease in summer monsoon precipitation in the SCS. The Leg 184 cores, along with the recent cores from the joint German-Chinese expedition *Monitor Monsoon* (Sarnthein et al., 1994), and the IMAGES III Cruise in 1997 provide for the first time systematic and high-quality material for paleomonsoon studies in the region (e.g., Wang et al., 1995a; Sun, 1996; Sun and Li, in press).

SCIENTIFIC OBJECTIVES

The long-term goals of Leg 184 are to determine the evolution and variability of the East Asian monsoon during the late Cenozoic and to improve our knowledge of the links between climate and tectonics. To meet these goals, Leg 184 has a number of major cruise and shore-based scientific objectives, including the following

(1) *Obtain continuous sequences of hemipelagic sediments that record the East Asian climate history during the late Cenozoic.*

The drilling plan takes advantage of the high hemipelagic sedimentation rates in the SCS to recover sections that are suitable for high-resolution stratigraphy. The seismic surveys reveal that different areas of the northern slope contain expanded sections of different ages. Our shipboard objective (see Proposed Sites and Operational/Drilling Plan sections) is to recover complete, high-accumulation rate sections for each age interval. For example, sedimentation rates on the continental slope vary from 0.7 to 15 cm/k.y. for the Holocene and from 1.3 to 31 cm/k.y. for the LGM, with the maximum values found near the mouth of the Pearl River and the paleo-Sunda River (Wang et al., 1995b). Recently, Core 17940 (20°07′N, 117°23′E, in a water depth of 1727 m; Sarnthein et al., 1994) in the northeast SCS, revealed a Holocene section nearly 7 m in thickness, which enables a temporal resolution of less than 15 yr (Fig. 8). The proposed drilling during Leg 184 will provide continuous records of monsoon variations back to the late Paleogene, enabling a comparison with the Indian monsoon records.

(2) *Establish records of monsoonal proxies for the SCS, including the variability of sediment properties, the rates of sediment accumulation, and the chemical, isotopic, and species variability of flora and fauna.*

On the basis of previous studies we anticipate that a number of sediment properties will exhibit variability related to monsoonal forcing (Figs. 3, 7, 8). Shipboard measurements will include core logging of magnetic susceptibility, bulk density, color reflectance, and natural gamma radiation, which along with faunal variations, can be related to monsoonal climates. Much of the previously identified monsoonal variability in tropical oceans is precessional (23 k.y.) in scale. We will construct initial splices and age models to identify the primary periodicity of the SCS records. By inference, strong precessional responses are likely related to monsoonal processes. Postcruise work will measure and refine the time series of chemical, isotopic, and faunal variability to give additional constraints on the relationship between sediment proxies and monsoonal variability.

(3) *Establish stratigraphic ties between the SCS marine record and the terrestrial record of China.*

Petroleum exploration and academic studies have accumulated a tremendous amount of Cenozoic paleoenvironmental information, particularly for on land and offshore China (Fig. 6). Because of the language barrier and commercial restrictions, little of these data have been available to the global scientific community. In addition, the poor stratigraphic control of the mostly nonmarine deposits has made it difficult to correlate the sediment records with the global paleoenvironmental history. The shipboard stratigraphy of the proposed sites will provide the first direct calibration of open-marine stratigraphy to the local and regional land-based stratigraphies, thereby linking them with the record of global environmental changes. Special attention will be paid to the timing of drastic changes in denudation/accumulation, monsoon intensification, seasonal cooling, and to the leads or lags between terrestrial and marine records.

(4) *Establish the relationship of East Asian monsoon variability with orbital and glacial forcing, and internal feedbacks of the climate system.*

The variability of monsoonal proxies and sedimentary characteristics identified on shipboard and in postcruise studies will be compared directly to time series of orbital changes to establish their coherency and phase (Fig. 3). Initial shipboard results should establish if the SCS monsoonal variations are consistent with orbital models of monsoonal variability. Postcruise research will be needed to expand and refine the sedimentary time series and perform more rigorous tests.

(5) *Compare the evolution of the East Asian monsoon in the SCS with the Indian monsoon in the Arabian Sea to identify common sources of causality.*

Given the identification of monsoonal indices in the SCS, especially for the winter monsoon, the SCS records will be compared to records of the summer monsoon from the ODP Arabian Sea sites. We anticipate that the summer monsoon signals should be similar (in phase) and that the winter monsoon will be stronger in the SCS. Since the winter monsoon reflects cooling over northern Asia, which is a function of both precession and obliquity, it may exhibit a more complex response than the summer monsoon. These studies will be initiated on shipboard, but most detailed comparisons will be made only after the final time series are established by postcruise research.

(6) *Test scenarios for the relationship between the Tibetan Plateau uplift, monsoon evolution, and global cooling.*

Land-based studies in China and marine-based ODP studies have postulated a variety of models for monsoon evolution (Table 1; Figs. 3, 4). The proposed drilling and logging program will calibrate the terrestrial records with those of the global ocean and make use of monsoonal proxies to establish the history of monsoon evolution in the SCS. Because uplift of the Tibetan Plateau is proposed to be responsible for both the late Cenozoic global cooling and for the intensification of the Asian monsoon, a comparison between records of monsoon intensity, denudation/accumulation rates, and climate cooling in the SCS will help test these hypotheses.

However, the relationships between tectonics, erosion, and climate are complex and highly nonlinear (see papers in Ruddiman, 1997). The tectonic control of the Asian monsoons, for example, is by no means limited to the plateau uplift. Only recently has the marine factor for monsoon evolution been discussed, but then only the role of the Paratethys was considered (Ramstein et al., 1997); whereas, the Western Pacific marginal seas should have more direct impact on the evolution of the East Asian monsoon. Drilling in the SCS will allow insights into the mechanisms of monsoon variation and will provide a new set of constraints concerning the links between tectonic uplift, weathering/erosion, and climate.

The shipboard identification of sediment characteristics and accumulation rates in the Miocene to Pleistocene sections of the SCS will likely distinguish between some models of monsoon evolution but will also raise questions or present new patterns to be deciphered. Significant postcruise research will be directed toward determining how the various sedimentary records are related to the models of HTC uplift and global cooling.

(7) *Improve our understanding of seasonality in the low-latitude SCS and how it relates to the strength and evolution of the winter monsoon.*
Late Neogene sections from the northern and southern part of the SCS will enable us to construct a history of the thermal gradient within the SCS (Fig. 7B). These paleotemperature data will provide information on when the winter monsoon began to develop large seasonality in the SCS and on the stability/variability of temperatures in the southern SCS, which lies within the Western Pacific Warm Pool.

Although seasonality is not necessarily related to monsoon circulation, intensification of monsoon circulation can trigger an increase in seasonality. The glacial increase in seasonality within the SCS is at least partly attributed to the strengthening of the East Asian winter monsoon. Aside from SST estimates, seasonality can also be recognized through abundance of index species in planktonic fauna.

PROPOSED SITES

Six primary and two alternate sites are proposed for drilling (Table 2). These fall into two groups: northeastern continental slope (Fig. 9) and southern slope (Fig. 10). A summary of the water depths for each site and the expected age/penetration is given in Figure 11.

1. Northeastern Continental Slope

Sites SCS-1 to 5 are located south of the Dongsha Islands in the northeast SCS (Fig. 9). The sites are designed to sample different water depths and to cover successive time intervals since the Oligocene (SCS-1: Pleistocene; SCS-2: middle Pliocene onward; SCS-3: Pliocene and Pleistocene; SCS-4: middle Miocene to Pliocene; SCS-5: Oligocene to Miocene). This suite of sites should provide the sections to identify and date the proposed stages of monsoon evolution in East Asia.

Site SCS-1

SCS-1 is targeted for 2050 m water depth, which is slightly above the sill depth of the Bashi Straits (2600 m). The location of Site SCS-1 is distinguished by extremely high sedimentation rates. The Holocene deposits in the nearby Core 17940 (20°07′N, 117°23′E, water depth 1727 m) reach almost 7 m in thickness, and Core MD 97.2.146 extends only to the oxygen stage 4/5 boundary at 38 m (C.Y. Huang, pers. comm., 1997). The summer monsoon cyclicity of 10^2 yr in the Holocene and the dry/humid cyclicity of 10^3 yr in the late Pleistocene found in Core 17940 (Wang et al., 1995a; Sun, 1996) indicate the great potential of this site in delivering high-resolution monsoon records for the Pleistocene. The target penetration of 450 m is anticipated to recover Quaternary sediments (~1 m.y.).

Site SCS-2

Proposed Site SCS-2 is downslope of SCS-1 at a water depth of 3190 m. This location has a lower sedimentation rate and is expected to provide a continuous record from the middle Pliocene to Pleistocene (Holocene). Because the sill depth of the Bashi Strait is located at ~2600 m, Sites SCS-1 and SCS-2 will also document the Quaternary changes in water mass characteristics across the sill, which is the only deep-water connection between the Pacific and the SCS. SCS-2 is targeted for 400 m penetration.

Site SCS-3C

Site SCS-3C is on the upper slope (water depth ~1265 m) near the base of the modern oxygen minimum zone (State Oceanic Administration, 1988; Haupt et al., 1994). This site is expected to provide a sequence of Pliocene and Pleistocene sediments that record changes in the intermediate water characteristics well above the sill depth. The variables of most interest are temperature and oxygen content, as well as surface-water conditions. Site SCS-3C is targeted for 300 m penetration.

Site SCS-4

Site SCS-4 is downslope of Site SCS-3C at a water depth of 2093 m. On the basis of seismic records, the proposed site should recover a middle Miocene to Pliocene sequence, which underlies relatively thin Pleistocene deposits. This site also lies above the current sill depth of the Bashi Straits and, along with SCS-5C, offers a Mio-Pliocene history of sill-related water-mass changes. SCS-4 is targeted for 520 m penetration.

Site SCS-5C

Site SCS-5C is located lower on the slope (3232 m) and is expected to recover an expanded Oligocene to Miocene section. On the basis of available seismic records and their correlation to Chinese reflector stratigraphy, SCS-5C is targeted for 700 m penetration. Given the expected accumulation rates and penetration depths, SCS-5C (and the alternate SCS-5D) are the only sites that will recover the Oligocene-Miocene history of the SCS, including the possible onset of the East Asian monsoon.

Alternate Sites SCS-5D and SCS-5E

Sites SCS-5D and SCS-5E are located about 65 and 20 km, respectively, northeast of Site SCS-5C. These alternate sites provide a somewhat expanded midsection compared to SCS-5C. They could be cored, if SCS-5C does not meet the expectations of a complete Oligocene-Miocene section.

2. Southern Slope

A southern continental slope SCS site is proposed to reveal the history of tropical East Asia and the Western Pacific Warm Pool (Fig. 10). Although the terrigenous deposits of the paleo-Sunda and Mekong Rivers provide a number of attractive targets in the southern part of the SCS, and piston cores in the region have high sedimentation rates and display high frequency climate variations, especially since the last glaciation. Safety considerations have entailed moving the site farther downslope (to the north) and limiting penetration. This southern location will be the only site within the Western Pacific Warm Pool and will provide a thermal contrast to the northern sites.

Site SCS-9

Proposed Site SCS-9 is at a water depth of 2830 m. Penetration is limited to 400 m, reaching the upper part of the upper Miocene.

OPERATIONAL/DRILLING STRATEGY

A number of operational, practical, and strategic factors were considered when developing the operational plan for Leg 184. Briefly, these include

1. Sites were selected to maximize recovery of different stratigraphic sections and different water depths. The northern continental margin sites comprise two transects: an eastern pair of sites that will focus on the Plio-Pleistocene section (Sites SCS-1 and SCS-2) at 2050 and 3190 m, respectively, and a western pair of sites that will focus on the Oligocene to Miocene section (Sites SCS-4 and SCS-5C) at 2093 and 3250 m, respectively.

2. All sites are considered to be first priority, but Site SCS-3C is considered at risk if operational time is limited. Site SCS-5C is considered to be the highest priority as it is the only site that will recover the Oligocene to Miocene section of the SCS. Alternate Site SCS-5D or 5E may become a higher priority than SCS-3C, if the coring results at SCS-5C do not satisfactorily recover the early history of the monsoon.

3. All sites will be triple piston cored (advanced hydraulic piston core [APC]) and extended core barrel (XCB) cored to total depth, with the possibility of double XCB if critical sections are not adequately recovered. The deeper sections of Site SCS-5C may be cored with the rotary core barrel system (RCB), if XCB penetration and recovery are not adequate.

4. Because of the limited number of seismic crossing lines at proposed sites, the *JOIDES Resolution* will conduct a seismic reflection survey (~2 to 2.5 days at Sites SCS-2, 3C, 4, and 5C and, if required, Sites SCS-5D and 5E) to verify that the proposed sites are safe and to provide a better structural framework for interpreting the sediment accumulation patterns. Coring at all but SCS-1 is contingent on safety panel approval, which will be based on the survey data.

5. Taking the above operational/coring considerations into account, the following sequence of operations is proposed: Depart Freemantle and transit to proposed Site SCS-9 and core. Then transit to Site SCS-1 and core. We will then conduct a seismic survey of northern sites to collect cross lines and select final site locations. Following the survey, we anticipate coring proposed Sites SCS-2, SCS-5C (or alternate), SCS-4, and SCS-3C in sequence before the final transit to Hong Kong.

6. ODP has requested Exclusive Economic Zone (EEZ) clearance for all proposed sites. Site SCS-9 requires drilling in waters that are claimed by several nations and EEZ clearance of this site may therefore be more problematic than for the northern sites. If SCS-9 should not get approved, the remaining time will be used to achieve the objectives, and maximize recovery, at the other sites, including SCS-3C.

WIRELINE LOGGING PLAN

The Leg 184 logging plan has been designed to provide (1) complete stratigraphic coverage, especially useful if core recovery is incomplete; (2) proxy data not available from core measurements, such as resistivity and yields of K, U, and Th; and (3) in situ sonic velocity for the construction of synthetic seismograms. All sites drilled to a depth greater than 400 m will be logged using the following three tool strings (see: http://www.ldeo.columbia.edu/BRG/new_kiosk.html for additional information on the tools):

A. "Triple-combo" toolstring, which includes: (1) the Dual Induction Tool (DITE) that measures resistivity from deep and shallow induction; (2) the Accelerator Porosity Sonde (APS) to measure porosity from epithermal neutron measurements; and (3) the Hostile Environment Litho-Density Sonde (HLDS) that measures bulk density from Compton scattering and general lithology from the photoelectric effect. The Hostile Environment Natural Gamma Ray Sonde (HNGS) that measures total natural gamma radiation and K, U, Th yields, and the LDEO Temperature Logging Tool (TLT) that measures borehole fluid temperature, are added to this toolstring.

B. "FMS-Sonic" toolstring which includes (1) the Formation Microscanner (FMS) that includes the General Purpose Inclinometry Tool (GPIT) and measures micro-resistivity at cm resolution; (2) the Dipole Sonic imager (DSI) that measures compressional and shear wave velocity, as well as cross dipole and Stoneley waveforms.

C. Geologic High-resolution Magnetic Tool (GHMT), which includes the Nuclear Magnetic Remanence Sonde (NMRS) to measure the total magnetic field, and the Susceptibility Measurement Sonde (SUMS) to measure the magnetic susceptibility from induction.

All tool names are trademarks of Schlumberger, except the TLT.

Use of the FMS-Sonic and GHMT toolstrings is contingent on hole conditions as estimated from the caliper measurements with the triple-combo string (always used for the first run), and the general course of the previous logging run. Estimated logging times for all three runs vary from 28 to 38 hr for the each of the Leg 184 sites.

SAMPLING STRATEGY AND SAMPLING PLAN

General

Sampling of the recovered cores will be subject to the rules described in the ODP Sample Distribution Policy (http://www-odp.tamu.edu/curation/sdp.htm). Based on the sample requests received by 15 November 1998, the Sample Allocation Committee (SAC) will prepare a temporary sampling plan, to be revised on the ship according to actual coring results. In the final shipboard sampling plan, sample requests will be closely linked to proposed postcruise research. Postcruise studies can also be proposed by shore-based investigators who do not participate in the cruise.

Logistics

The core sampling logistics are three-fold: (1) shipboard sampling for shipboard measurements, (2) shipboard sampling for postcruise studies, and (3) postcruise sampling for postcruise studies. Some sampling for shipboard measurement of ephemeral properties must occur immediately, before stratigraphic correlation information is available (see below). These measurements include organic geochemistry for safety monitoring (free gas and 20 cm^3 sediment samples), interstitial-water chemistry (whole-round of 5-15 cm length), and moisture content (10 cm^3 sediment). In addition, core catchers will be analyzed for biostratigraphic datums.

Shipboard sampling for postcruise studies will be kept to a reasonable minimum, trying to balance the need for an initial set of samples for immediate postcruise laboratory work against the need for avoiding redundant or "frenzy" sampling before the composite section and splice are constructed (see below). The SAC may decide to sample the upper few cores on the ship because high-porosity sediments could be disturbed during transport to the Texas A&M University (TAMU) core repository. Samples that need to be frozen or sealed for shore-based analysis also must be taken onboard. All shipboard scientists will participate in shipboard sampling according to a shift schedule.

Because of the large number of requested samples that are expected, most investigators will be encouraged to participate in a postcruise sampling meeting in the core repository ~4 months postcruise. The ODP repository staff will fill the remaining requests.

Core Material

Most of the material to be recovered is expected to be hemipelagic mud with moderate carbonate content and low abundance of organic material. Sedimentation rates are expected to range typically between 2-20 cm/k.y., although some sites may have substantially higher rates.

Stratigraphic Coverage, MCD, and the Splice

Complete stratigraphic coverage will be attempted at all sites. Because coring gaps occur, even between successive cores with nominally 100% recovery, complete sections will be achieved by triple coring with the APC system (typically the uppermost 150-250 m). Double XCB coring of the deeper intervals may be considered, depending on the priority of the section and the available time. In addition to ensuring complete coverage, multiple-hole coring also provides significantly more core material for sampling.

The shipboard stratigraphic correlators will be responsible for constructing a composite depth section for each site in near-real time. The "meters composite depth" (mcd) scale correlates the cores from multiple holes based on core logging data. All investigations from any hole can then be linked by using the mcd scale. A shipboard "splice" will be defined by the correlators, which is one continuous stratigraphic core section for a site composed of core intervals from different holes. The splice can be used by most investigators for sampling. However, because of the short distance from the final site to port, the "mcd splice" for the last few sites may not be available for sampling until the postcruise sampling party.

Special Circumstances

At any time during the cruise, the SAC will determine whether special circumstances for a certain interval warrant either a sampling moratorium or solicitation of a special sampling program.

REFERENCES

ASCOPE, 1981. *Tertiary Sedimentary Basins of the Gulf of Thailand and South China Sea: Stratigraphy, Structure and Hydrocarbon Occurrences*. ASCOPE, Jakarta.

Anderson, D., and Webb, R.S., 1994. Ice-age tropics revisited. *Nature*, 367:23-24.

Bian, Y., Wang, P., and Zheng, L., 1992. Deep-water dissolution cycles of late Quaternary planktonic foraminifera in the South China Sea. *In* Ye, Z., and Wang, P. (Eds.), *Contributions to Late Quaternary Paleoceanography of the South China Sea*. Qingdao Ocean University Press, 261-273 (in Chinese, with English abstract).

Briais, A., Patriat, P., and Tapponnier, P., 1993. Updated interpretation of magnetic anomalies and seafloor spreading stages in the South China Sea: implications for the Tertiary tectonics of Southeast Asia. *J. Geophys. Res.*, 98:6299-6328.

Cerling, T., 1997. Late Cenozoic Vegetation Change, Atmospheric CO_2, and Tectonics. *In* Ruddiman, W.F. (Ed.), *Tectonic Uplift and Climate Change*, Plenum, New York, 313-327.

Chen, L., Zhu, G., Luo, H., He, J., Dong, M., and Feng, Z., 1991. *The East Asian Monsoons*. China Meteorological Press, Beijing (in Chinese).

Clemens, S.C., and Prell, W.L., 1991. Late Quaternary forcing of Indian Ocean summer-monsoon winds: A comparison of Fourier model and general circulation model results. *J. Geophys. Res.*, 96:22,683-22,700.

Clemens, S.C., Murray, D.W., and Prell, W.L., 1996. Nonstationary Phase of the Plio-Pleistocene Asian Monsoon. *Science,* 274:943-948.

Clemens, S.C., Prell, W.L., Murray, D., Shimmield, G., and Weedon, G., 1991. Forcing mechanisms of the Indian Ocean monsoon. *Nature*, 353:720-725.

CLIMAP Project Members, 1976. The surface of the ice-age Earth. *Science*, 191:1131-1137.

CLIMAP Project Members, 1981. Seasonal reconstructions of the Earth's surface at the last glacial maximum. *Geol. Soc. of Am., Map and Chart Ser.* MC-36.

Cochran, J.R., 1990. Himalayan uplift, sea level, and the record of Bengal Fan sedimentation at the ODP Leg 116 sites. *In* Cochran, J.R., Stow, D.A.V. (Eds.) *Proc. ODP, Sci. Results,* 116: College Station, TX (Ocean Drilling Program), 397-414.

Copeland, P., Harrison, T.M., Kidd, W.S.F., Ronghua, X., and Yuquan, Z., 1987. Rapid early Miocene acceleration of uplift in the Gangdese Belt, Xizang (southern Tibet), and its bearing on accommodation mechanisms of the India-Asia collision. *Earth Planet. Sci. Lett*., 86:240-252.

Ding, Z.L., Sun, J.M., Yang, S.L., and Liu, T.S., 1998. Preliminary magnetostratigraphy of a thick eolian red-clay loess sequence at Lingtai, the Chinese Loess Plateau. *Geophys. Res. Lett.*, 25:1225-1228.

Harrison, T.M., Copeland, P., Kidd, W.S.F., and Yin, A., 1991. Raising Tibet. *Science,* 255:1663-1670.

Hastenrath, S., and Greischar, L., 1993. The monsoonal heat budget of the hydrosphere-atmosphere system in the Indian Ocean sector. *J. Geophys. Res.*, 98:6869-6881.

Hastenrath, S., 1991. Climate dynamics of the tropics. Kluwer Academic Publishers, Boston.

Haupt, B., Wiesner, M., & Sarnthein, M., 1994. CTD profiles and bottom water temperatures in the South China Sea (SONNE-95 Cruise). Reports, Geol.-Paleont. Inst., Univ. Kiel, No.68:181-194.

Hayes, D.E., Nissen, S.S., Buhl, P., Diebold, J., Yao, B., Zeng, W., and Chen, Y., 1995. Throughgoing crustal faults along the northern margin of the South China Sea and their role in crustal extension. *J. Geophy. Res.*, 100:22435-22446.

Huang, L., 1997. Calcareous nannofossil biostratigraphy in the Pearl River Mouth Basin, South China Sea, and Neogene reticulofenestrid coccoliths size distribution pattern. *Marine Micropaleontology*, 32:31-57.

Jennerjahn, T.C., Liebezeit, G., Kempe, S., Xu, L.Q., Chen, W.B., and Wang, H.K., 1992.Particle flux in the northern South China Sea. *In* Jin, X., Hudrass, H.R., Pautot, G. (Eds.), *Marine Geology and Geophysics of the South China Sea*. China Ocean Press, Beijing, 228-235.

Jiang, Z., Lin, Z., Li, M., et al., 1994. Tertiary in Petroliferous Regions of China, VIII. The North Continental Shelf Region of South China Sea. Petroleum Industry Press, (in Chinese).

Jin, Q. (Ed.), 1989. Geology and oil-gas resources of the South China Sea. Geological Publishing House, Beijing, (in Chinese).

Jin, X., 1992. Tectogenesis and origin of northern South China Sea. *In* Jin, X., Hudrass, H.R., Pautot, G. (Eds.), *Marine Geology and Geophysics of the South China Sea*. China Ocean Press, Beijing, 1-9.

Kalnay, E. et al., 1996. The NCEP/NCAR 40-Year Reanalysis Project. *Bull. Amer. Meteorol. Soc.*, 77:437-471.

Kump, L., and Arthur, M., 1997. Global chemical erosion during the Cenozoic: Weatherability balances the budgets. *In* Ruddiman, W.F. (Ed.), *Tectonic Uplift and Climate Chang*e, Plenum, New York, 172-203.

Liu, T., and Ding, M., 1982. Pleistocene stratigraphy and Plio/Pleistocene boundary in China. *Quaternary Geology and Environment of China*. China Ocean Press, Beijing, 1-6.

Liu, T., and Ding, Z., 1993. Stepwise coupling of monsoon circulations to global ice volume variations during the late Cenozoic. *Global and Planetary Chang*e, 7:119-130.

Miao, Q., Thunell, R.C., and Anderson, D.M., 1994. Glacial-Holocene carbonate dissolution and sea surface temperatures in the South China and Sulu seas. *Paleoceanography,* 9:269-290.

Molnar, P., England, P., and Martinod, J., 1993. Mantle dynamics, uplift of the Tibetan Plateau, and the Indian monsoon. *Reviews of Geophysics,* 31:357-396.

Morley, J.J., and Heusser, L.E., 1997. Role of orbital forcing in East Asian monsoon climates during the last 350 kyr: Evidence from terrestrial and marine climate proxies from core RC14-99. *Paleoceanography*, 12:483-494.

Murakami, T., 1987. Orography and monsoons. *In* Fien, J., and Stephens, P. (Eds.), *Monsoons*, Wiley, New York, 331-364.

Prell, W.L., 1984a. Monsoonal climate of the Arabian Sea during the Late Quaternary: a response to changing solar radiation. *In* Berger, A.L., Imbrie, J., Hays, J., Kukla, G., and Saltzman, B. (Eds.), *Milankovitch and Climate,* D. Riedel, Hingham, 349-366.

______, 1984b. Variation of monsoonal upwelling: A response to changing solar radiation. *In* Hansen, J., and Takahashi T. (Eds.), *Climate Processes and Climate Sensitivity*, Amer. Geophys. Union, 48-57.

Prell, W.L., and Kutzbach, J.E., 1987. Monsoon variability over the past 150,000 years. *J. Geophys. Res.*, 92:8411-8425.

Prell, W.L., and Kutzbach, J.E., 1992. Sensitivity of the Indian monsoon to forcing parameters and implications for its evolution. *Nature*, 360:647-652.

______, 1997. The impact of Tibet-Himalayan elevation on the sensitivity of the monsoon climate system to changes in solar radiation. *In* Ruddiman, W.F., (Ed.), *Tectonic Uplift and Climate Change*, Plenum, New York, 172-203.

Prell, W.L., Murray, D.W., Clemens, S.C., and Anderson, D.M., 1992. Evolution and variability of the Indian Ocean summer monsoon: Evidence from the western Arabian Sea drilling program. *In* Duncan, R.A. (Ed.), *The Indian Ocean: A Synthesis of Results from the Ocean Drilling Program*, Amer. Geophys. Union, Washington D.C., 447-469.

Prell, W.L., Niitsuma, N., et al., 1991. *Proc. ODP, Sci. Results*, 117: College Station, TX (Ocean Drilling Program).

Quade, J., Cerling, T.E., and Browman, J.R., 1989. Dramatic ecologic shift in the late Miocene of northern Pakistan, and its significance to the development of the Asian monsoon. *Nature*, 342:163-166.

Ramstein, G., Fluteau, F., Besse, J., and Joussaume, S., 1997. Effect of orogeny, plate motion and land-sea distribution on Euroasian climate change over the past 30 million years. *Nature*, 386:788-795.

Raymo, M.E., 1994. The Himalayas, organic carbon burial, and climate in the Miocene. *Paleoceanography*, 9:399-404.

Raymo, M.E., Ruddiman, W.F., and Froelich, P.N., 1988. The influence of late Cenozoic mountain building on ocean geochemical cycles. *Geology*, 16:649-653.

Rea, D.K., 1992. Delivery of Himalayan sediment to the northern Indian Ocean and its relation to global climate, sea level, uplift, and seawater strontium. *In* Duncan, R.A., Rea, D.K., Kidd, R.B., von Rad, U., and Weissel, J.K. (Eds.), *Synthesis of Results from Scientific Drilling in the Indian Ocean.* Am. Geophys. Union, Washington, D.C. Geophysical Monograph 70, 387-402.

Ru, K., Zhou, D., and Chen, H., 1994. Basin evolution and hydrocarbon potential of the northern South China Sea. *In* Zhou, D., Liang, Y., Zeng, C. (Eds.), *Oceanology of China Seas*, Kluwer, 2:361-372.

Ruddiman, W.F. (Ed), 1997. *Tectonic Uplift and Climate Change*. Plenum, New York.

Ruddiman, W.F., and Kutzbach, J.E., 1989. Forcing of late Cenozoic Northern Hemisphere climate by plateau uplift in Southern Asia and the American West. *J. Geophys. Res.*, 94:18409-18427.

Sarnthein, M., Pflaumann, U., Wang, P.X., and Wong, H.K. (Eds.), 1994. Preliminary Report on Sonne-95 Cruise "Monitor Monsoon" to the South China Sea. *Reports, Geol.- Palaont. Inst. Univ. Kiel*, 68.

Schärer, U., Tapponnier, P., Lacassin, R., Leloup, P.H., Zhong, D. and Ji, S., 1990. Intraplate tectonics in Asia: a precise age for large-scale Miocene movement along the Ailao Shan--Red River shear zone, China. *Earth and Planet. Sci. Lett.*, 97:65-77.

Sorocko, F., Sarnthein, M., Erlenkeuser, H., Lange, H., Arnold, M. and Duplessy, J.C., 1993. Centry-scale events in monsoonal climate over the past 24,000 years. *Nature*, 364:322-324.

State Oceanic Administration, China, 1988. Atlas of environment and resource complex investigations in the central part of the South China Sea. China Ocean Press, Beijing (in Chinese).

Stuijts, I., Newsome, J.C., and Flenley, J.R., 1988. Evidence for late Quaternary vegetational change in the Sumatran and Javan highlands. *Review of Palaeobotany and Palynology*, 55:207-216.

Sun, X., 1996. Environmental changes of the northern South China Sea since the last 30 k.y. based on pollen data of deep sea Core 17940-2 (Abstract). *IGC-30 Abstracts*, 2:254.

Sun, X., and Li, X., in press. Pollen records of the last 37 ka in deep-sea core 17940 from the northern slope of the South Cina Sea. *Marine Geology*.

Thunell, R.C., Miao, Q., Calvert, S.E., and Pedersen, T.F., 1992. Glacial-Holocene biogenic sedimentation patterns in the South China Sea: productivity variations and surface water CO_2. *Paleoceanography*, 7:143-162.

Wang, L., and Wang, P., 1990. Late Quaternary paleoceanography of the South China Sea: glacial-interglacial contrasts in an enclosed basin. *Paleoceanography*, 5:77-90.

Wang, L., Pflaumann, U., and Sarnthein, M., 1995a. High-resolution sediment records of climatic change in the South China Sea during the last 30,000 years (Abstract). *ICP-V Program and Abstracts*, 175-176.

Wang, L., Sarnthein, M., Erlenkeuser, H., Grimalt, J., Grootes, P., Heilig, S., Ivanova, E., Kienast, M., Pelejero, C., and Pflaumann, U., in press. East Asian monsoon climate during the late Pleistocene: High-resolution sediment records from the South China Sea. *Marine Geology*.

Wang, P., 1990. Neogene stratigraphy and paleoenvironments of China. *Palaeogeogr., Palaeoclimatol., Palaeoecol.*, 77:315-334.

______, 1997. Late Cenozoic environment evolution in China: marine factors and records. *Proceedings of the Fourth International Conference on the Evolution of the East Asian Environment, January 3-6, 1995*, Hong Kong University, 264-274.

______, in press. Response of West Pacific marginal seas to glacial cycles: Paleoceanographic and sedimentological features. *Marine Geology*.

Wang, P., Min, Q., Bian, Y., and Feng, W., 1986. Planktonic foraminifera in the continental slope of the northern South China Sea during the last 130,000 years and their paleoceanographic implications. *Acta Geologica Sinica* (Trial English Edition), 60:1-11.

Wang, P., Wang, L., Bain, Y., and Jian, Z., 1995b. Late Quaternary paleoceanography of the South China Sea: surface circulation and carbonate cycles. *Marine Geology*, 127:145-165.

Wang, P., Bradshaw, M., Ganzei, S.S., Tsukawaki, S., Hanssan, K.B., Hantoro, W.S., Poobrasert, S., Burne, R., Zhao, Q., and Kagami, H., 1997. West Pacific marginal seas during last glacial maximum: amplification of environmental signals and its impact on monsoon climate. *30th International Geological Congress, Proceedings*, VSP, the Netherlands, 13:65-85.

Webster, P.J., Magana, V.O., Palmer, T.N., Shukla, J., Tomas, R.A., Yanai, M., and Yasunari, T., 1998. Monsoons: Processes, predictability, and the prospects for prediction, in the TOGA decade. *J. Geophys. Res.*, 103:14,451-14,510.

Webster, P.J., 1987. The elementary monsoon. *In*, Fien, J. and Stephens P., (Eds.), *Monsoons*, Wiley, New York, 3-32.

______, 1994. The role of hydrological processes in ocean-atmosphere interactions. *Rev. Geophys.*, 32:427-476.

Wu, J., 1994. Evaluation and models of Cenozoic sedimentation in the South China Sea. *Tectonophysics*, 235:77-98.

Zheng, L., Ke, J., Winn, K., Stoffers, P., 1993. Carbonate sedimentation cycles in the northern South China Sea during the late Quaternary. *In* Zheng, L., and Chen, W. (Eds.), *Contributions to Sedimentation Process and Geochemistry of the South China Sea.* China Ocean Press, 109-123 (in Chinese, with English abstract).

FIGURE CAPTIONS

Figure 1. Climatology of the summer and winter monsoon circulation. Surface winds for the **(A)** winter (January) and **(B)** summer (July) seasons along with areas of high (H) and low (L) pressure, and precipitation (6 and >9 mm/day contours) for the **(C)** winter (January) and **(D)** summer (July) seasons. The pressure gradients and resulting wind and precipitation patterns reflect the land-sea heating contrasts, which are a function of solar radiation, elevation, and land-surface boundary conditions. Monthly data for 1990-1997 from NOAA NCEP-NCAR CDAS-1 (Kalnay, et al., 1996).

Figure 2. Regional setting of the South China Sea (SCS) and the two areas of proposed coring locations (see Figs. 9 and 10 for closeups ofnorthern and southern drilling areas, respectively). Note that the SCS is connected to adjacent seas and the Pacific by shallow sills, with the deepest being the Bashi Strait (BS; 2600 m water depth).

Figure 3. Summary of some of the marine and terrestrial observations that indicate an intensification of the monsoon in the late Miocene (10-8 Ma) and a model simulation of a possible evolution of monsoon runoff. **A.** Abundance of planktonic foraminifer *Globigerina bulloides* and radialarian *Actinoma* spp. that indicate active upwelling induced by southwest monsoonal winds (from ODP Site 722, Arabian Sea). **B.** Oxygen and carbon isotopes measured in pedogenic carbonates from Pakistan indicating more seasonal climates and a decrease in atmospheric CO_2 possibly due to monsoon related weathering (data from Quade et al., 1989). **C.** Normalized, mean terrigenous sediment flux to the northern Indian Ocean that indicates active uplift and fluvial deposition in the late Miocene (from Rea, 1992). **D.** A model simulation of monsoon runoff using the Molnar model for uplift history (11-8 Ma) and the coupled effects of elevation change and orbitally-induced solar radiation changes (from Prell and Kutzbach, 1997).

Figure 4. The migration of the arid zones (black areas) in China during the Cenozoic. **A.** Paleocene. **B.** Neogene. **C.** The location of sites with paleobotanic and/or lithologic data (from Sun and Wang, pers. comm., 1998) that define the terrestrial climates.

Figure 5. Tectonic setting of the South China Sea. **A.** Major tectonic elements of the northern and central parts of the South China Sea. Thick dotted line outlines the Central Basin with selected magnetic anomaly lineaments. Thin dotted and solid lines are isobaths of 200 m and 2000 m (Hayes et al., 1995). Thick dashed box corresponds to Figure 3. **B.** Geological framework of the northern margin of the South China Sea (Ru et al., 1994). YGHB = Yinggehai Basin; QDNB = Qiongdongnan Basin; BBWB = Baibiwan Basin; PRMB = Pearl River Mouth Basin; SWTB = Southwest Taiwan Basin. Leg 184 sites are located south of Dongsha Island on the continental margin between the Pearl River Mouth Basin and the South China Sea Basin.

Figure 6. A composite stratigraphy from industrial wells in the eastern part of the Pearl River Mouth Basin, which lies on the shelf and uppermost continental slope northwest of the northern sites (PRMB in Fig. 5; see Fig. 9 for bathymetry). These wells provide the seismic reflector sequence and general age structure that we hope to correlate to the more marine ODP sites on the slope. Note the nonmarine sequence beginning from late Oligocene (modified from Jiang et al., 1994).

Figure 7. Conditions in the Western Pacific marginal seas at the last glacial maximum (LGM). **A.** Areas of emergent shelf (black) at the LGM (Wang et al., 1997). Area A = East China Sea Shelf; Area B = Sunda Shelf or the Great Asian Bank; Area C = Sahul Shelf or the Great Australian Bank. **B.** The patterns of SST seasonality (summer SST minus winter SST) in the South China Sea and its adjacent Western Pacific and marginal seas at the LGM (Wang, in press).

Figure 8. East Asian monsoon climate change in the northern SCS during the last glacial cycle from a core recovered during the SONNE 17940 cruise. The plots show are, from top to bottom, total grain size mode; clay content; stable oxygen isotope values from *Globigerinoides ruber*, and for reference, the oxygen isotope record from theGISO2 ice core. EHPB = Early Holocene/Pre Boreal; Y.D. = Younger Dryas; B/A = Boelling/Alleroed; O.D. = Oldest Dryas (data from Wang et al., in press).

Figure 9. Bathymetry of the northern margin of the SCS and the location of sites proposed for Leg 184 (solid circles). Contours are every 100 m. See Table 2 for exact locations and depths.

Figure 10. Bathymetry of the southern margin of the SCS and the location of sites proposed for Leg 184 (solid circles). Contours are every 100 m. See Table 2 for exact locations and depths.

Figure 11. Summary of water depths and expected ages of the intervals to be drilled during Leg 184. Also shown are the present day critical sill, lysocline, and CCD depths. Proposed Sites SCS-1 and SCS-2 form a Pliocene-Pleistocene depth transect, and SCS-4 and SCS-5C form a Miocene depth transect.

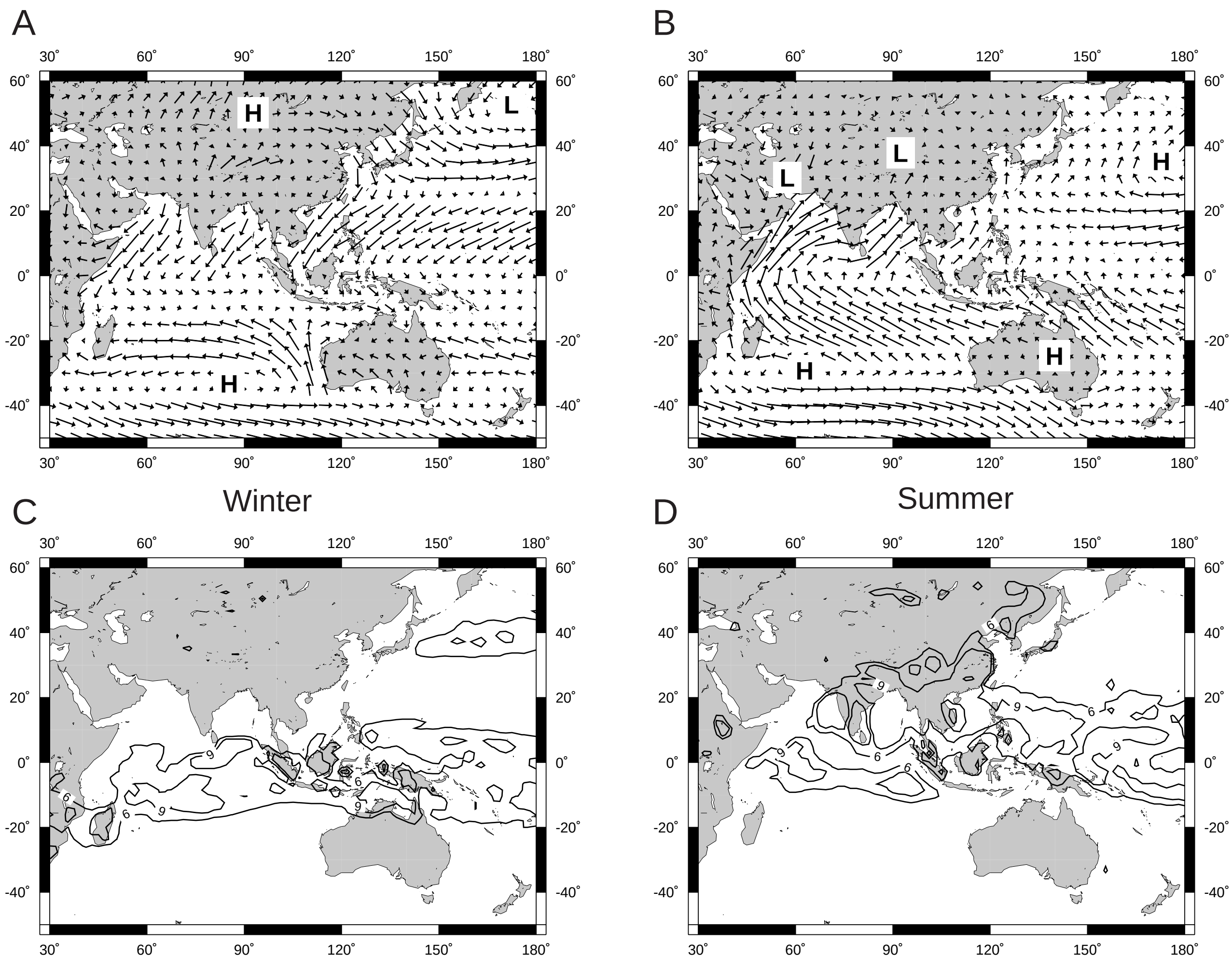

Figure 1. Climatology of the summer and winter monsoon circulation. Surface winds for the **(A)** winter (January) and **(B)** summer (July) seasons along with areas of high (H) and low (L) pressure areas, and precipitation (6 and >9 mm/day contours) for the **(C)** winter (January) and **(D)** summer (July) seasons. The pressure gradients and resulting wind and precipitation patterns reflect the land-sea heating contrasts, which are a function of solar radiation, elevation, and land-surface boundary conditions. Monthly data for 1990-1997 from NOAA NCEP-NCAR CDAS-1 (Kalnay et al, 1996).

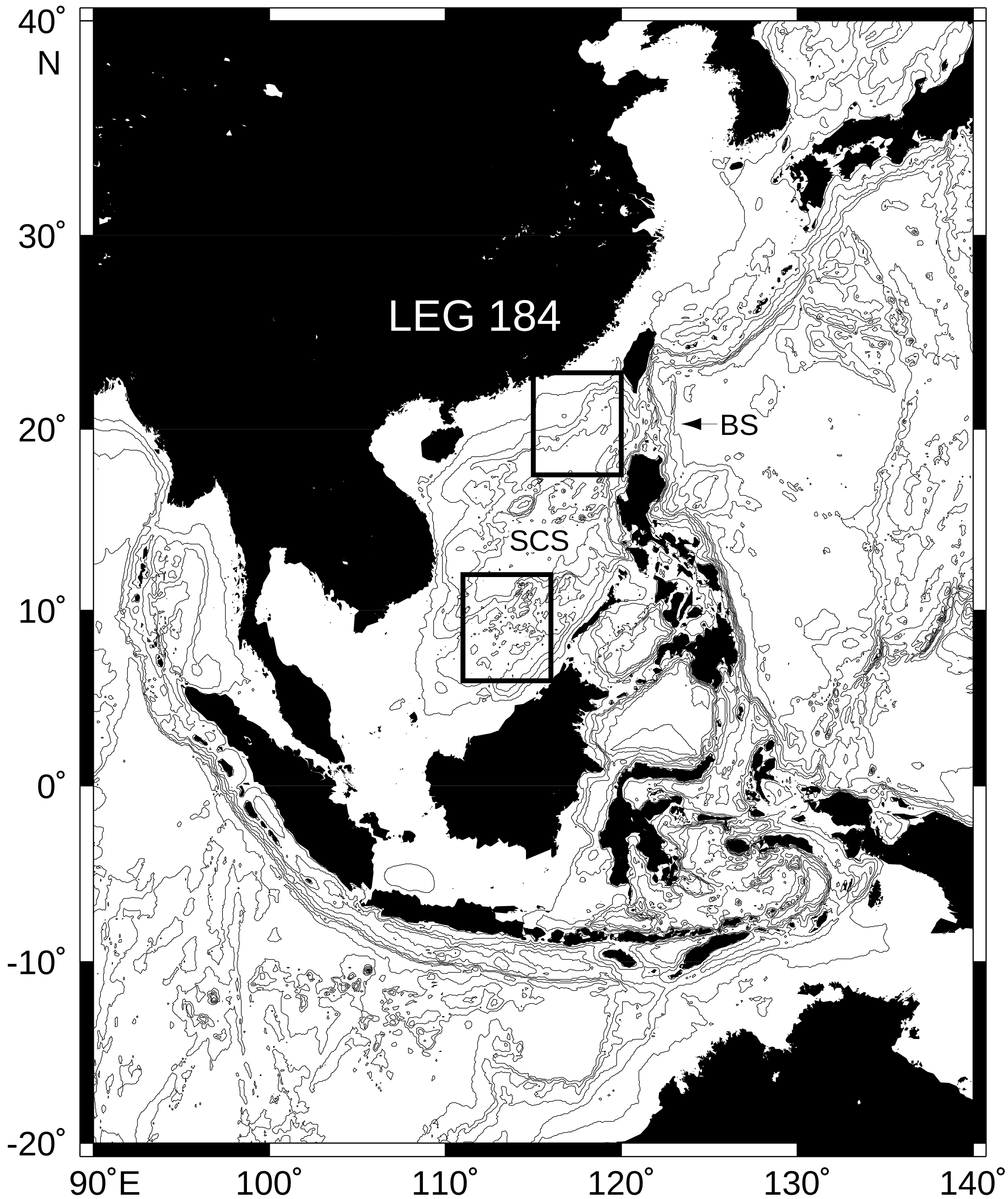

Figure 2. Regional setting of the South China Sea (SCS) and the two areas of proposed coring locations (see Figs. 9 and 10 for closeups of northern and southern drilling areas, respectively). Note that the SCS is connected to adjacent seas and the Pacific by shallow sills, with the deepest being the Bashi Strait (BS; 2600 m water depth).

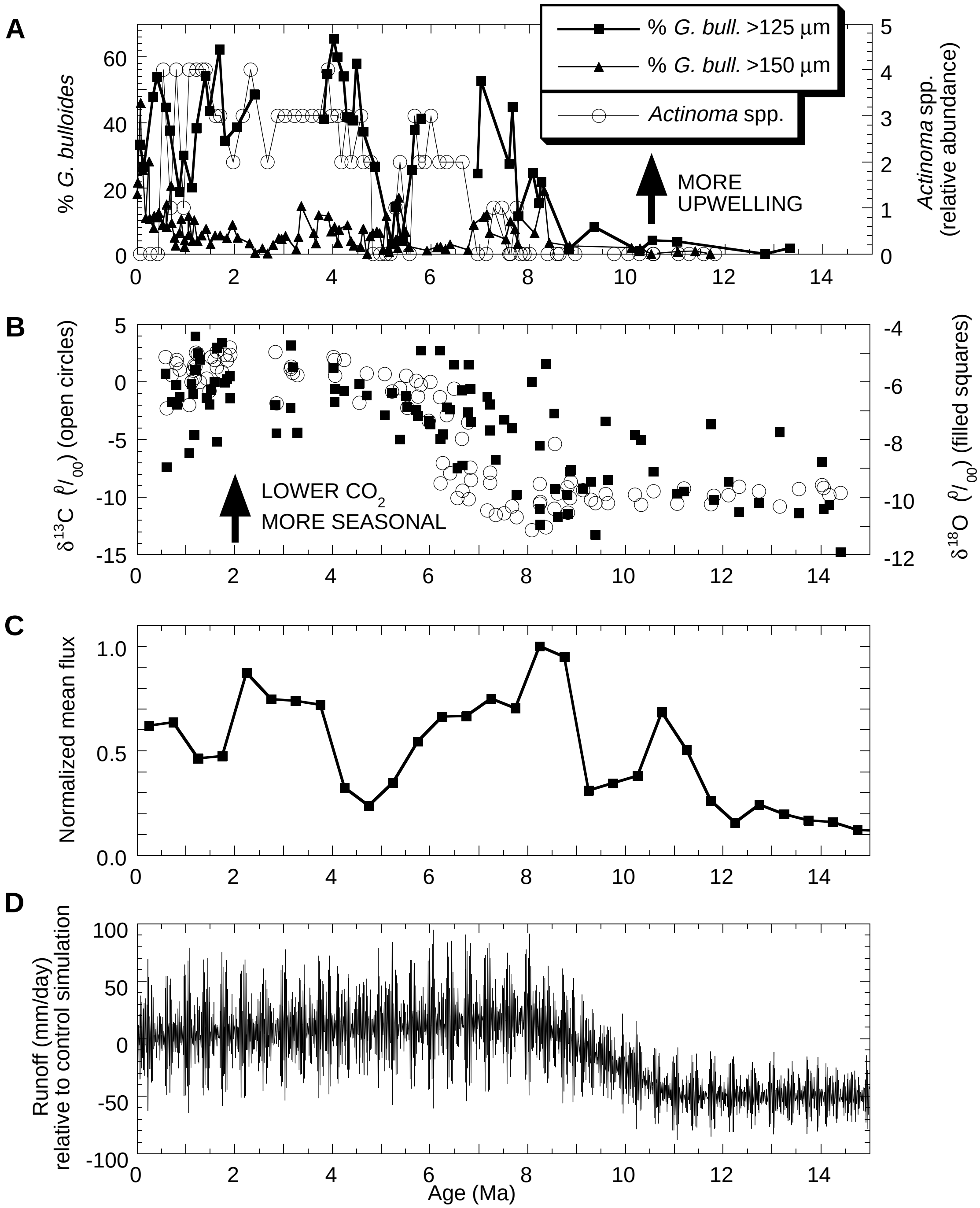

Figure 3. Summary of some of the marine and terrestrial observations that indicate an intensification of the monsoon in the late Miocene (10-8 Ma) and a model simulation of a possible evolution of monsoon runoff. **A.** Abundance of planktonic foraminifer *Globigerina bulloides* and radiolarian *Actinoma* spp. that indicate active upwelling induced by southwest monsoonal winds (from ODP Site 722, Arabian Sea). **B.** Oxygen and carbon isotopes measured in pedogenic carbonates from Pakistan indicating more seasonal climates and a decrease in atmospheric CO_2 possibly due to monsoon related weathering (data from Quade et al., 1989). **C.** Normalized, mean terrigenous sediment flux to the northern Indian Ocean that indicates active uplift and fluvial deposition in the late Miocene (from Rea, 1992). **D.** A model simulation of monsoon runoff using the Molnar model for uplift history (11-8 Ma) and the coupled effects of elevation change and orbitally-induced solar radiation changes (from Prell and Kutzbach, 1997).

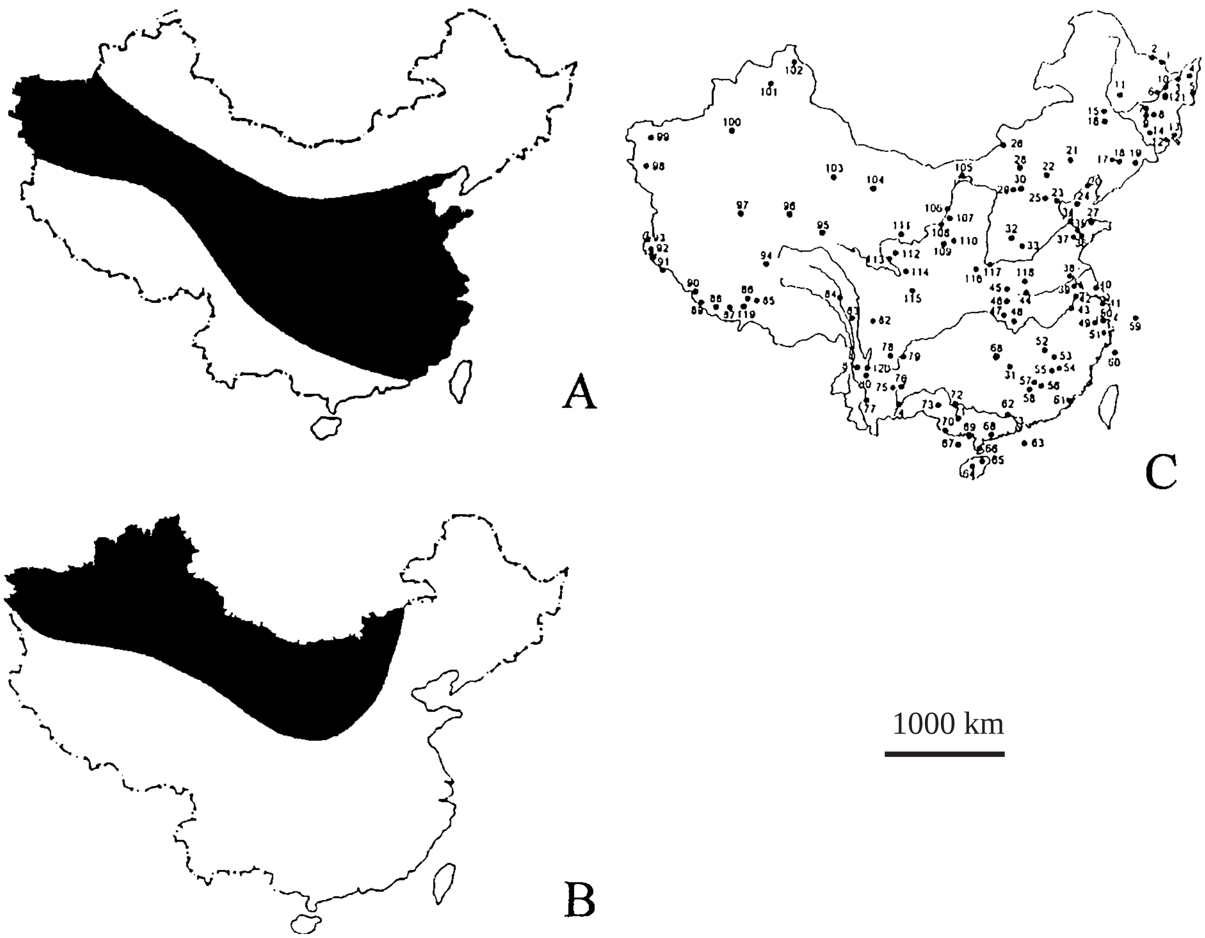

Figure 4. The migration of the arid zones (black areas) in China during the Cenozoic. A. Paleocene, and B. Neogene. C. The location of sites with paleobotanic and/or lithologic data (from Sun and Wang, in prep.) that define the terrestrial climates.

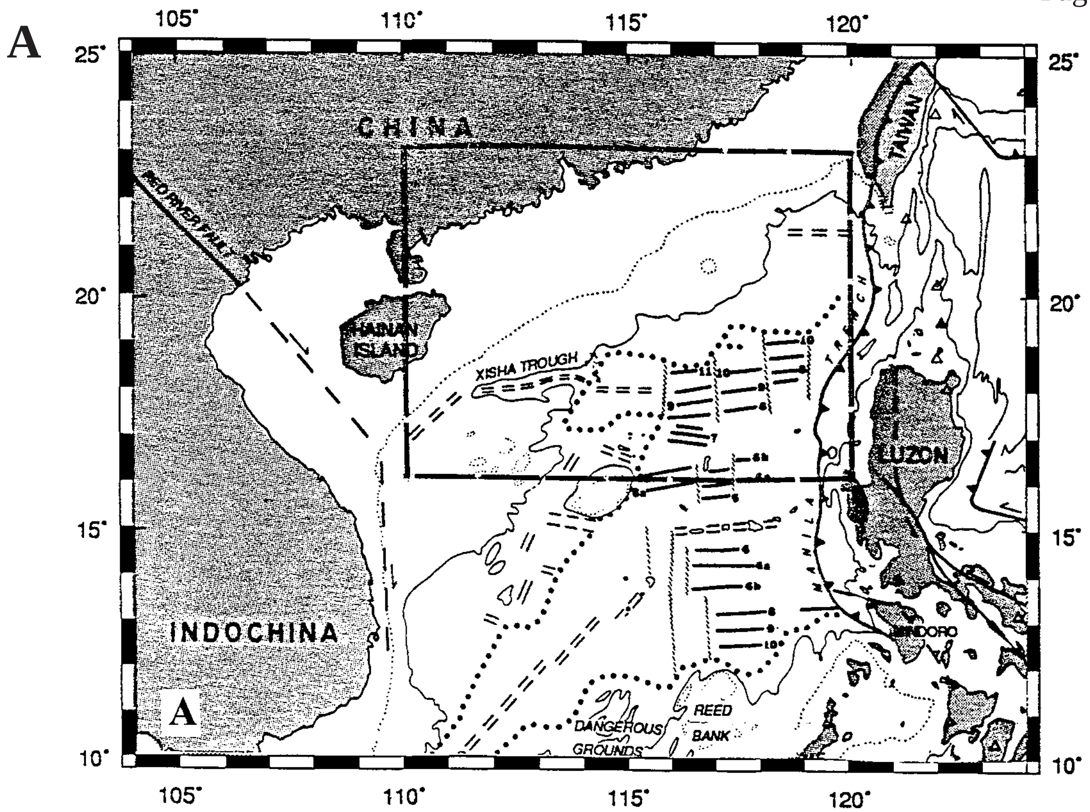

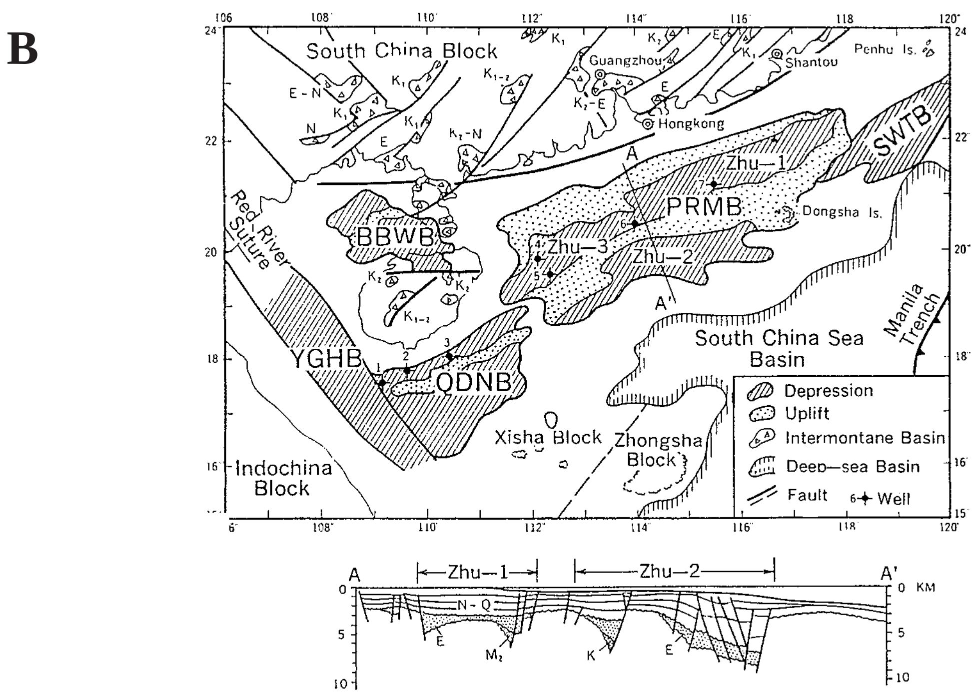

Figure 5. Tectonic setting of the South China Sea. **A.** Major tectonic elements of the northern and central parts of the South China Sea. Thick dotted line outlines the Central Basin with selected magnetic anomaly lineaments. Thin dotted and solid lines are isobaths of 200 m and 2000 m (Hayes et al., 1995). Thick dashed box corresponds to Figure 3. **B.** Geological framework of the northern margin of the South China Sea (Ru et al., 1994). YGHB = Yinggehai Basin; QDNB = Qiongdongnan Basin; BBWB = Baibiwan Basin; PRMB = Pearl River Mouth Basin; SWTB = Southwest Taiwan Basin. Leg 184 sites are located south of Dongsha Island on the continental margin between the Pearl River Mouth Basin and the South China Sea Basin.

Period	Epoch		Formation	Thickness m	Lithology	Seism. Reflector	Fossil Zone Foram.	Fossil Zone Nanno.	Description
Q	Pleisto.			55.8~444		T$_N$	N23 | N22	NN21 | NN19	Marine grey-greyish muds with fine sands, intercalated with non-marine muds, sands and partly sandy gravel in upper part
Ng	Plio.		Wanshan	0~541		T$_1$	N21 | N18	NN18 | NN12	Marine grey-greyish green mudstone with thin siltstone
Ng	Mio.	u	Yuehai	55.8~677.5		T$_2$	N17 | N16	NN11 | NN10	Marine greyish green mudstone, grey siltstone with non-marine thick-bedded sandstone
Ng	Mio.	m	Hanjiang	306~1153.5		T$_4$	N15 | N9	NN9 | NN5	Alternation of non-marine greyish green mudstone, grey siltstone, sandstone with marine greyish mudstone and siltstone
Ng	Mio.	l	Zhujiang	270~1022		T$_6$	N8 | N4B	NN4 | NN1 (upper)	Upper part: marine mudstone, siltstone and reef limestone Middle part: alternations of marine greyish mudstone, limestone and alluvial sandstone and mudstone Lower part: alluvial sandstone and mudstone with local tuff lenses
Pg	Oligo.	u	Zhuhai	0~875		T$_7$	N4A | P22	NN1 (lower) | NP24	Alluvial sandstone and mudstone with thin marine facies interbeds, replacing by marine sandstone and mudstone southward
Pg	Oligo.	l	Enping	0~1111.5					Upper part: non-marine dark grey mudstone, grey sandstone and thin coal seams, with marine interbeds in the southmost part of the basin containing nannofossils of NP24/23 Lower part: non-marine thick sandstone and thin dark shale
Pg	Eo.	u	Enping			T$_8$			Upper part: lacustrine and alluvial grey, greyish brown mudstone and sandstone, with a thin marine mudstone in the northeast part of the basin containing NP15 nannofossils Lower part: arkos conglomerate, sandstone and muddy sandstone with thin shale and coal beds
Pg	Eo.	m	Wenchan	0~432		T$_9$			
Pg	Eo.	l	Shenhu	0~958					Light grey tuff with quartz porphyry and thin mudstone intercalations, covered by a layer of felsophyre. In some part of the basin alternating sandstones and mudstones
Pg	Paleo.		Shenhu			T$_g$			
Mesozoic									Late Mesozoic granites, partly metamorphic or effusive rocks

Figure 6. A composite stratigraphy from industrial wells in the eastern part of the Pearl River Mouth Basin, which lies on the shelf and uppermost continental slope northwest of the northern sites (PRMB in Fig. 5; see Fig. 9 for bathymetry). These wells provide the seismic reflector sequence and general age structure that we hope to correlate to the more marine ODP sites on the slope. Note the nonmarine sequence beginning from late Oligocene (modified from Jiang et al., 1994).

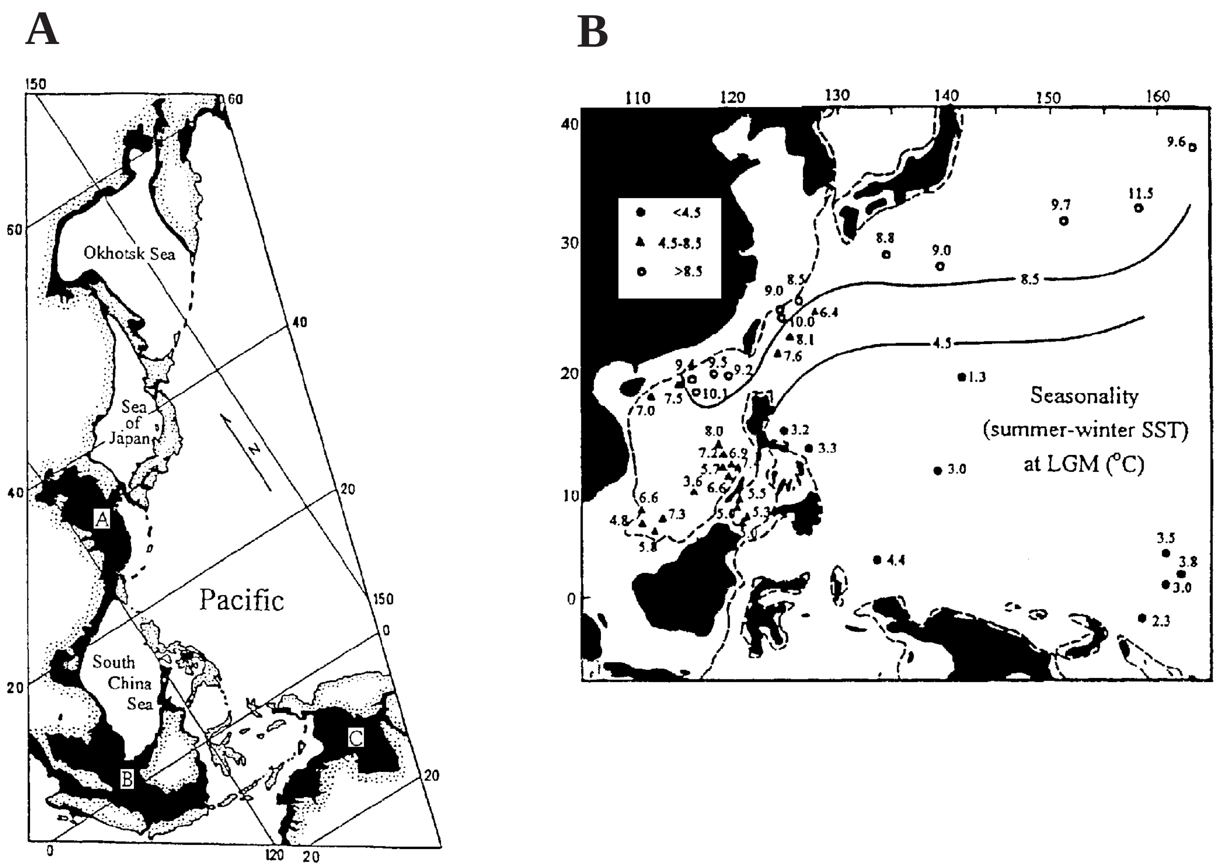

Figure 7. Conditions in the Western Pacific marginal seas at the last glacial maximum (LGM). **A.** Areas of emergent shelf (black) at the LGM (Wang et al., 1997). Area A = East China Sea Shelf; Area B = Sunda Shelf or the Great Asian Bank; Area C = Sahul Shelf or the Great Australian Bank. **B.** The patterns of SST seasonality (summer SST minus winter SST) in the South China Sea and its adjacent Western Pacific and marginal seas at the LGM (Wang, in press).

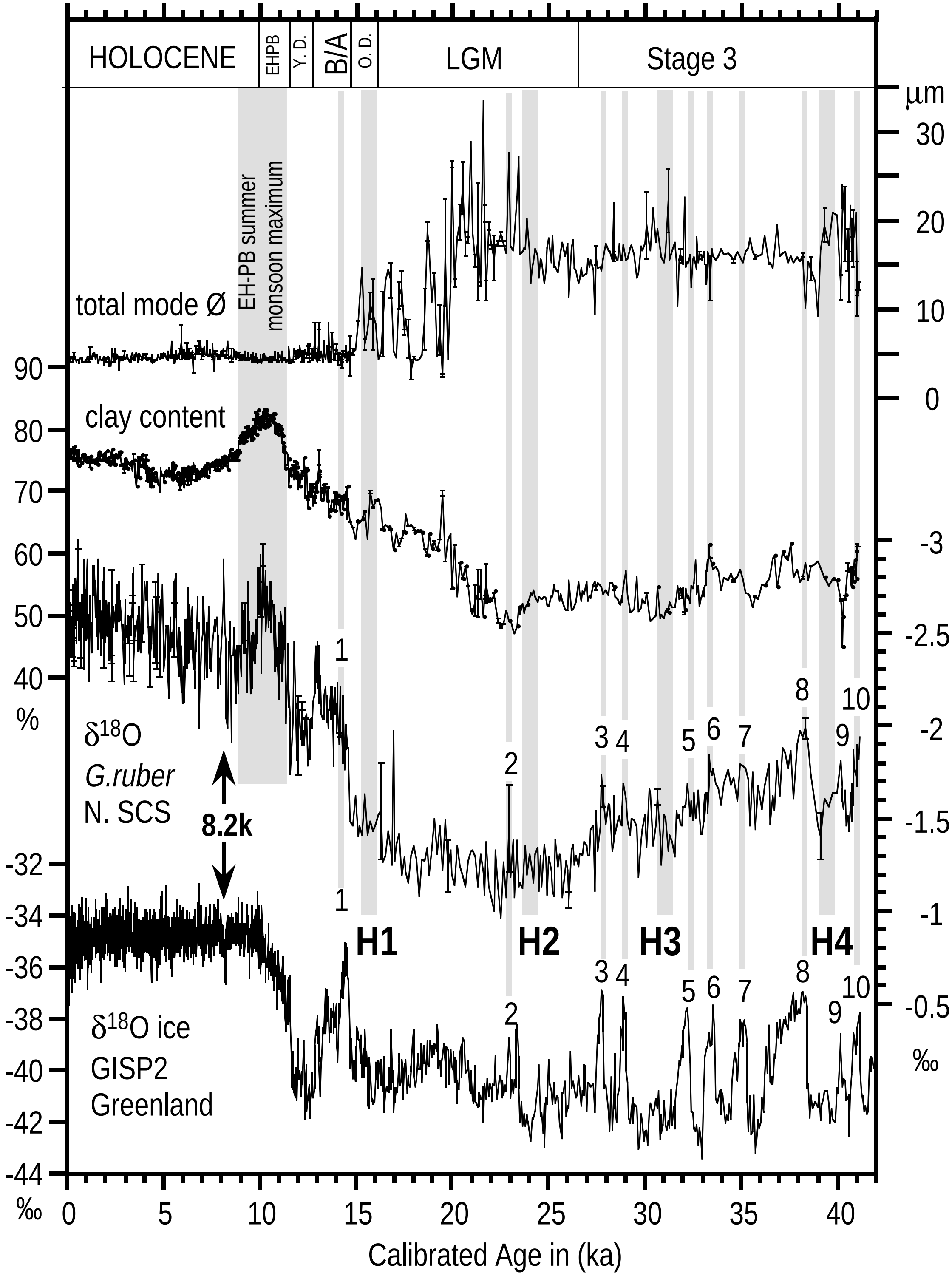

Figure 8. East Asian monsoon climate change in the northern SCS during the last glacial cycle from a core recovered during the SONNE 17940 cruise. The plots shown are, from top to bottom: total grain size mode; clay content; stable oxygen isotope values from *Globigerinoides ruber;* and for reference, the oxygen isotope record from the GISP2 ice core. EHPB = Early Holocene/Pre Boreal; Y.D. = Younger Dryas; B/A = Boelling/Alleroed; O.D. = Oldest Dryas; LGM = Last glacial maximum. Data from Wang et al. (in press).

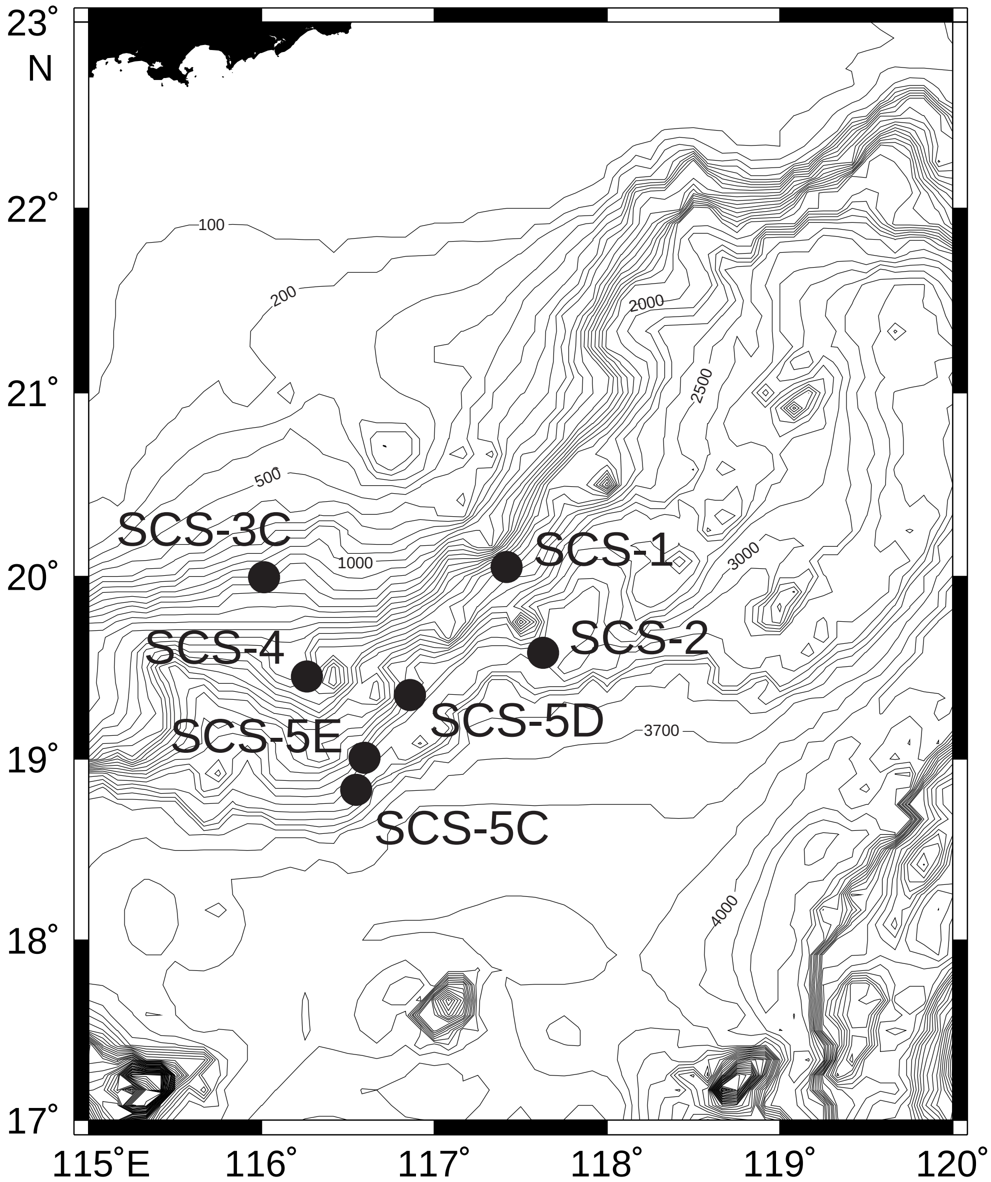

Figure 9. Bathymetry of the northern margin of the SCS and the location of sites proposed for Leg 184 (solid circles). Contours are every 100 m. See Table 2 for exact locations and depths.

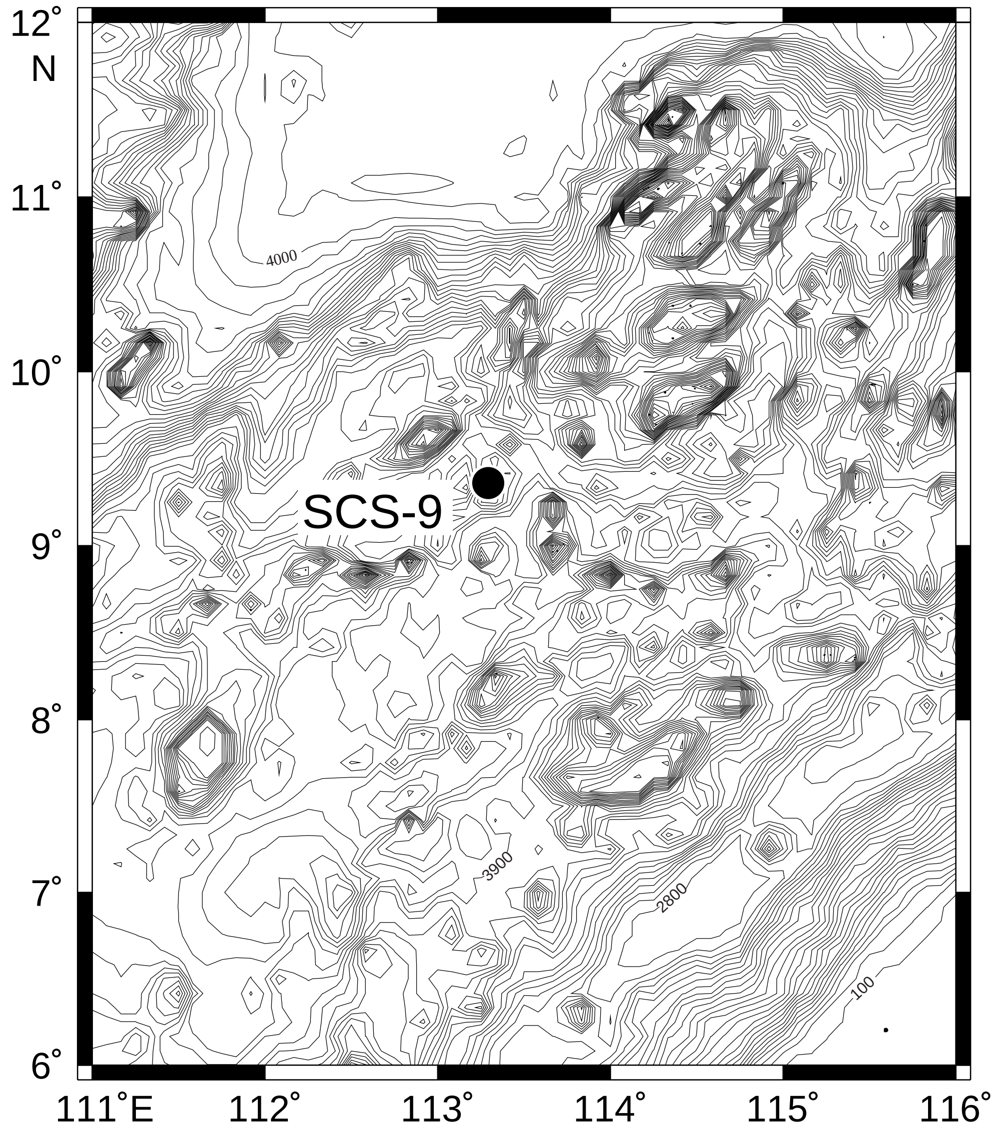

Figure 10. Bathymetry of the southern margin of the SCS and the location of proposed site SCS-9 (solid circle). Contours are every 100 m. See Table 2 for exact location and depth.

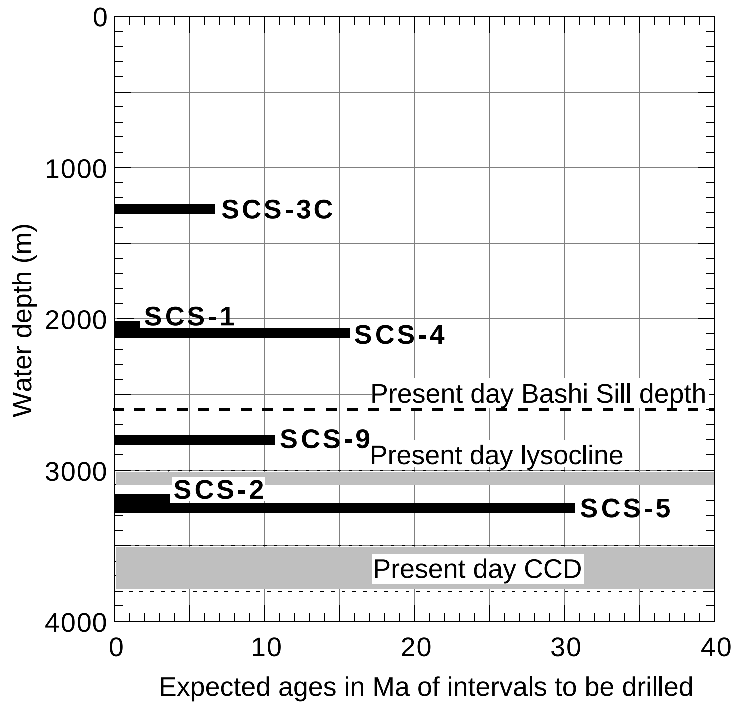

Figure 11. Summary of water depths and expected ages of the intervals to be drilled during Leg 184. Also shown are the present day critical sill, lysocline, and CCD depths. Proposed sites SCS-1 and SCS-2 form a Pliocene-Pleistocene depth transect, and SCS-4 and SCS-5C form a Miocene depth transect.

TABLE 2. LEG 184 Operations Plan and Time Estimate

Site No.	Location Lat/Long	Water Depth	Operations Description	PPSP (mbsf)	Transit (days)	Drilling (days)	Logging (days)	Total On-site
PRIMARY SITES								
Freemantle			Transit 2766 nmi from Freemantle to SCS-9 @ 10.5 kt		11.0			
SCS-9	09°21.72'N	2830 m	Triple APC to 250 mbsf then deepen one hole	400		5.5	1.2	6.7
	113°17.10'E		with the XCB to 400 mbsf. Wireline log					
			Transit 864 nmi from SCS-9 to SCS-1 @ 10.5 kt		3.4			
SCS-1	20°03.18'N	2050 m	Triple APC to 250 mbsf then deepen one hole	450		4.6	1.2	5.8
	117°25.14'E		with the XCB to 450 mbsf. Wireline log					
			Transit/Survey 285.7 nmi from SCS-1 to SCS-2 @ 6.0 kt		2.0			
SCS-2	19°35.04'N	3190 m	Triple APC to 250 mbsf then deepen one hole	400		5.6	1.3	6.9
	117°37.86'E		with the XCB to 400 mbsf. Wireline log					
			Transit 76 nmi from SCS-1 to SCS-5C @ 10.5 kt		0.3			
SCS-5C	18°49.73'N	3232 m	Triple APC to 250 mbsf, then deepen one hole	700		9.8	1.6	11.3
	116°32.93'E		to 450 mbsf 'w/ XCB. Change BHA and drill ahead					
			to 450 mbsf, RCB core to 700 mbsf, Wireline log					
			Transit 40 nmi from SCS-5C to SCS-4 @ 10.5 kt		0.2			
SCS-4	19°27.24'N	2093 m	Triple APC to 250 mbsf then deepen one hole	520		5.0	1.3	6.3
	116°15.84'E		with the XCB to 520 mbsf. Wireline log					
			Transit 29 nmi from SCS-4 to SCS-3C @ 10.5 kt		0.1			
SCS-3C	19°59.76'N	1265 m	Single APC hole to 300 mbsf.	300		1.2		1.2
	116°0.90'E							
Hong Kong			Transit 175 nmi from SCS-3C to Hong Kong @ 10.5 kt		0.8			
					17.8	**31.6**	**6.5**	**38.2**
					TOTAL DAYS:	**56.0**		
					Alt for	**Drilling (days)**	**Logging (days)**	
ALTERNATE SITES								
SCS-5D	19°20.94'N	2682 m	Same as 5C	700	5C	9.0	1.6	10.6
	116°51.66'E							
SCS-5E	19°0.36'N	3143 m	Same as SCS-5D	770	5C	9.7	1.6	11.3
	116°35.88'E							

DATE=8/25/98 **FILE: I:\ DATA \ DSD_INFO \LEGS\184\PRO484 Rev.XLS**

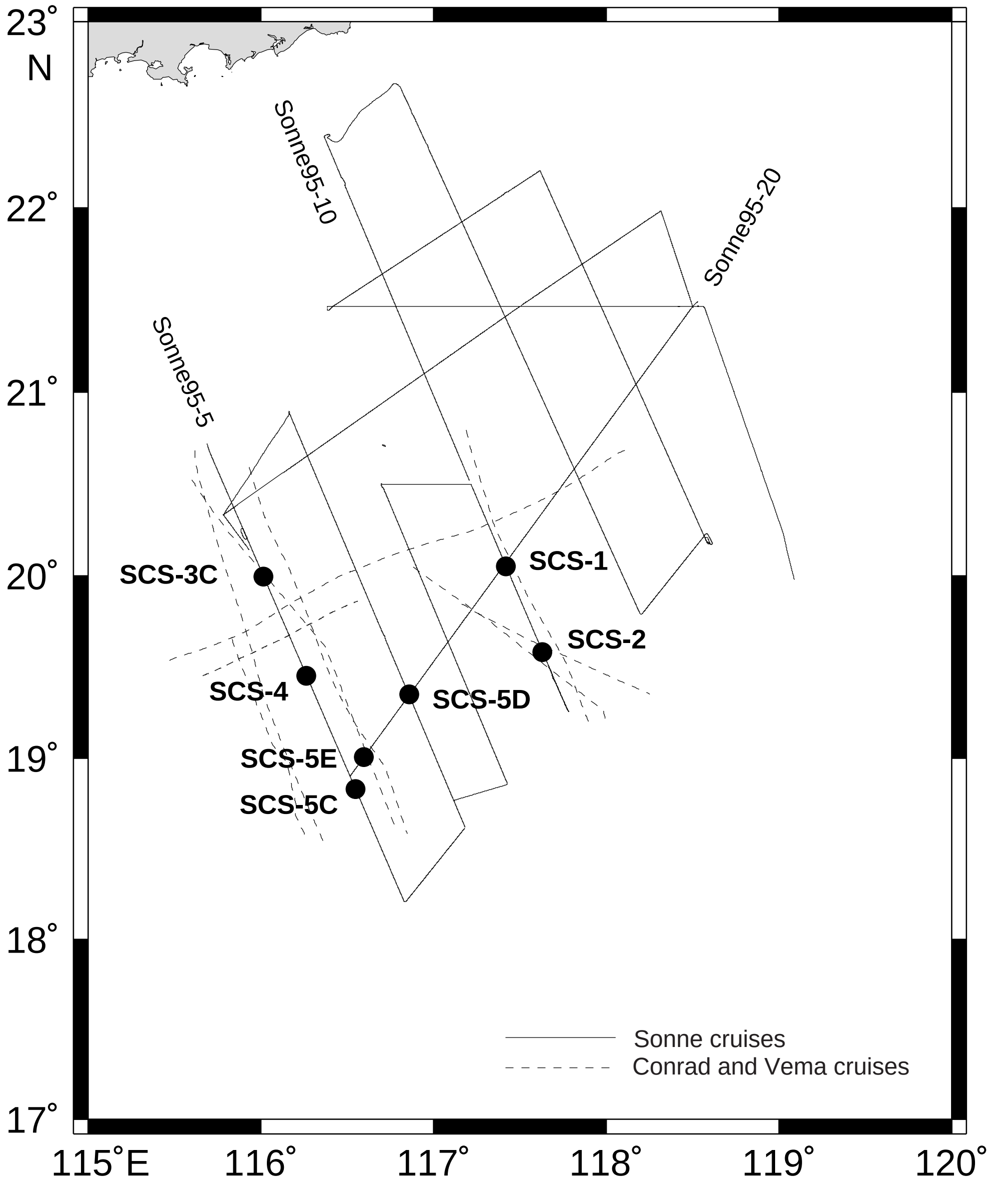

Seismic survey lines and proposed site locations in the northern SCS drilling area. Area shown corresponds to that in Figure 2 (overview) and Figure 9 (bathymetry). The lengths of the seismic sections shown in the site descriptions correspond approximately to the size of the filled circles representing each site.

Proposed Site SCS-1

Line SO95-10, CDP 9700 (4:20)

Water depth: 2050 m

Approved penetration depth: 450 mbsf

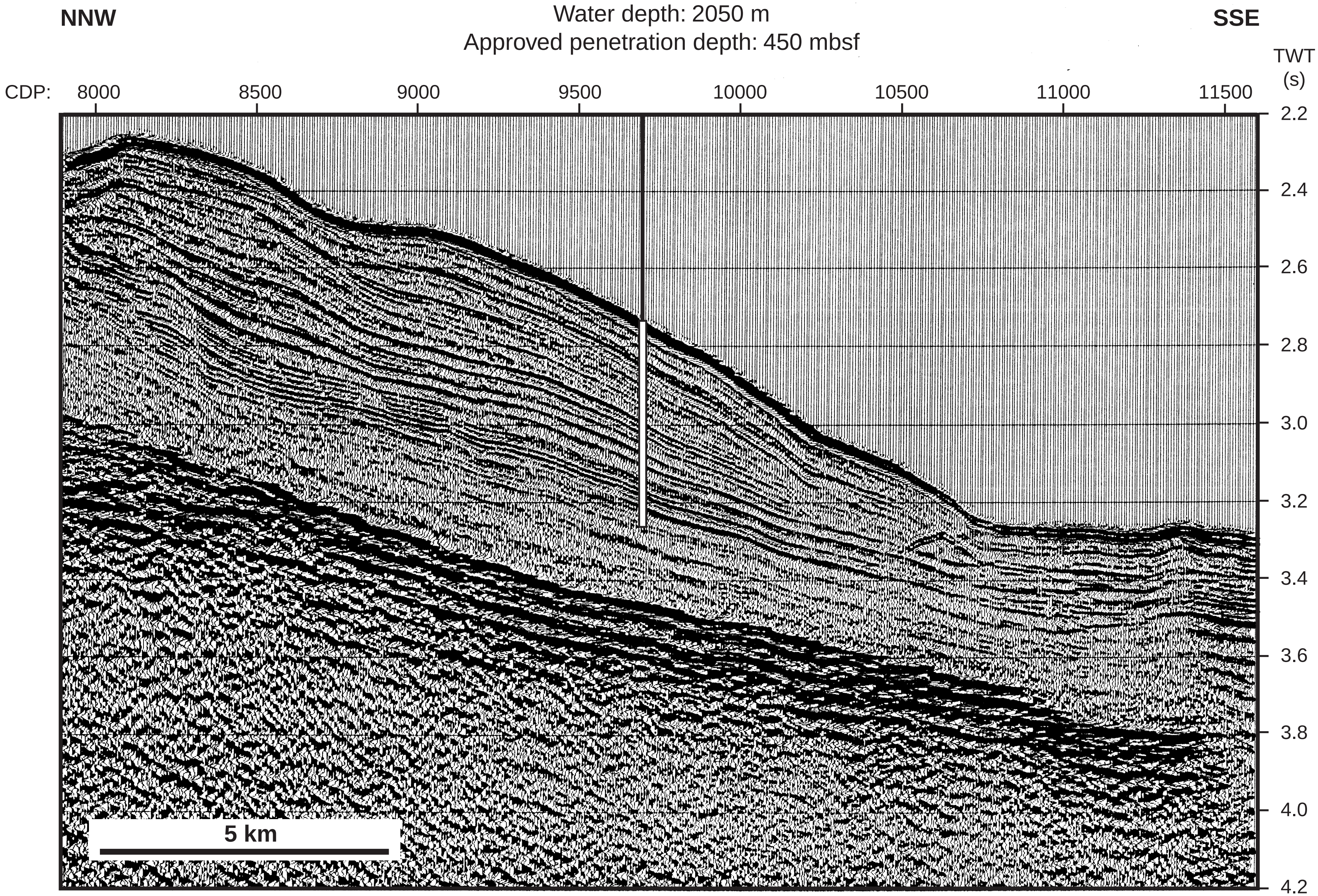

Proposed Site SCS-1 (projected)
Line SO95-20, CDP 3430 (4:02)
Water depth: 2050 m
Approved penetration depth: 450 mbsf

NE SW

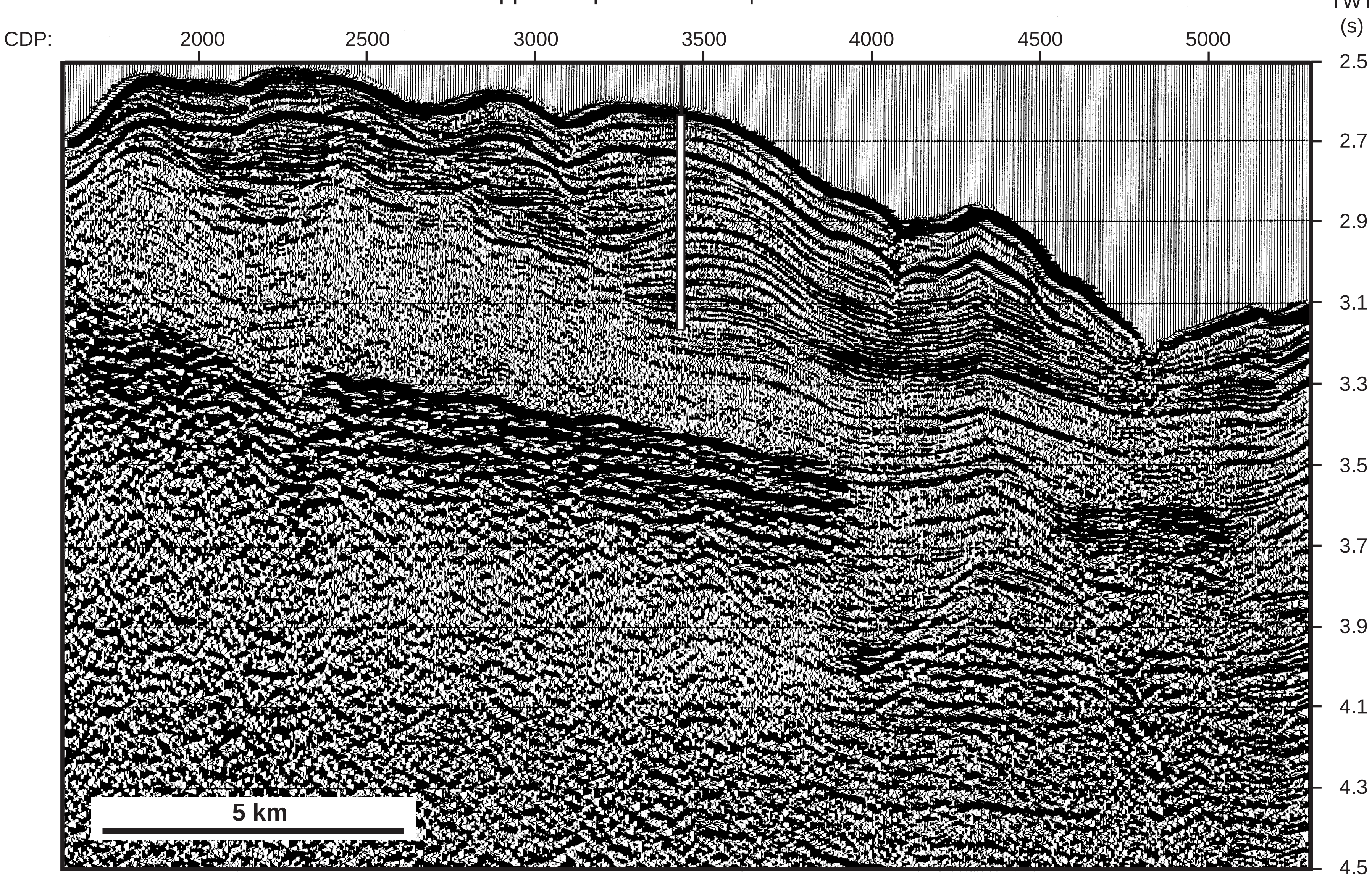

SITE SUMMARIES

Site: SCS-1

Priority: 1
Position: 20°03.18´N, 117°25.14´E
Water Depth: 2050 m
Sediment Thickness: ~760 m
Approved Maximum Penetration: 450 m
Seismic Coverage: Intersection of SO-95 Profiles 10 and 20

Objectives

1. To recover a continuous sequence of high accumulation rate hemipelagic sediments to reconstruct the Pleistocene paleomonsoon history on a millenial (or higher resolution) time scale.

2. To identify the time scales of variability for sediment characteristics and accumulation rates. The time series of sediment variability will be compared with records of orbital-scale and higher frequency records from ice cores, marginal seas, and terrestrial deposits.

3. To establish a high-resolution record of SST changes associated with the winter monsoon and for comparison to the SST history of the southern SCS.

Drilling Program: Triple APC to refusal, XCB to 450 mbsf

Logging and Downhole Operations: Triple-combo, GHMT, and sonic-FMS

Nature of Rock Anticipated: Hemipelagic mud

Proposed Site SCS-2

Line SO95-10, CDP 4680 (11:10)
Water depth: 3190 m
Approved penetration depth: 400 mbsf

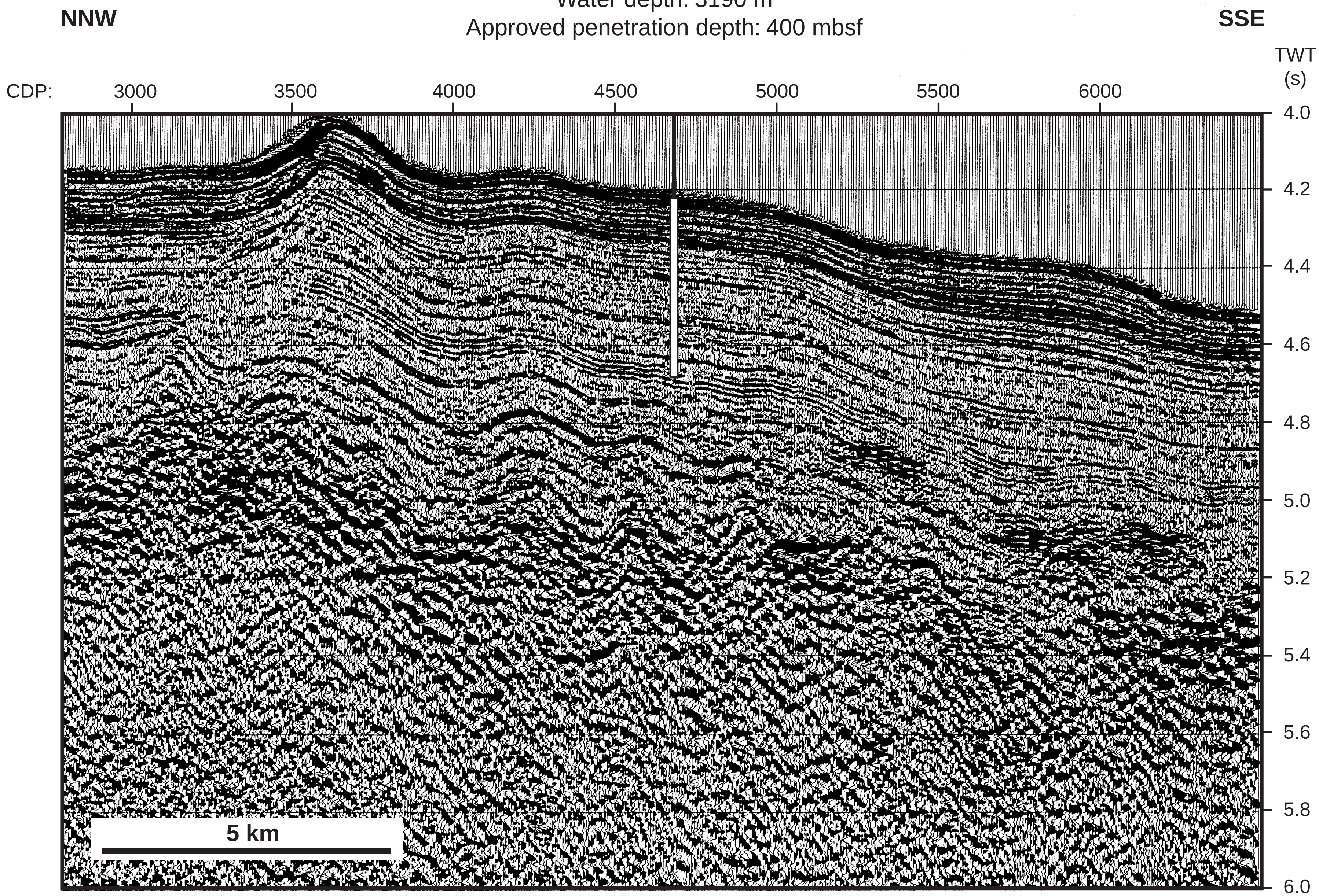

Site: SCS-2

Priority: 1
Position: 19°35.04'N, 117°37.86'E
Water Depth: 3190 m
Sediment Thickness: ~870 m
Approved Maximum Penetration: 400 m
Seismic Coverage: Intersection of SO-95 Profile 10 and Vema Profile 3068

Objectives:

1. To recover a continuous sequence of hemipelagic sediments to reconstruct the middle Pliocene to Pleistocene/Holocene paleomonsoon history.

2. To establish if the SCS records an intensification of the winter monsoon during the Pliocene, consistent with the development of loess in China.

3. To establish if the summer monsoon is intensifying or weakening during the Plio-Pleistocene.

Drilling Program: Triple APC to refusal, XCB (or double XCB) to 400 mbsf

Logging and Downhole Operations: Triple-combo, GHMT, and sonic-FMS

Nature of Rock Anticipated: Hemipelagic mud and mudstone

Proposed Site SCS-3C

Line SO95-5, CDP 15600 (10:10)

Water depth: 1265 m

Approved penetration depth: 300 mbsf

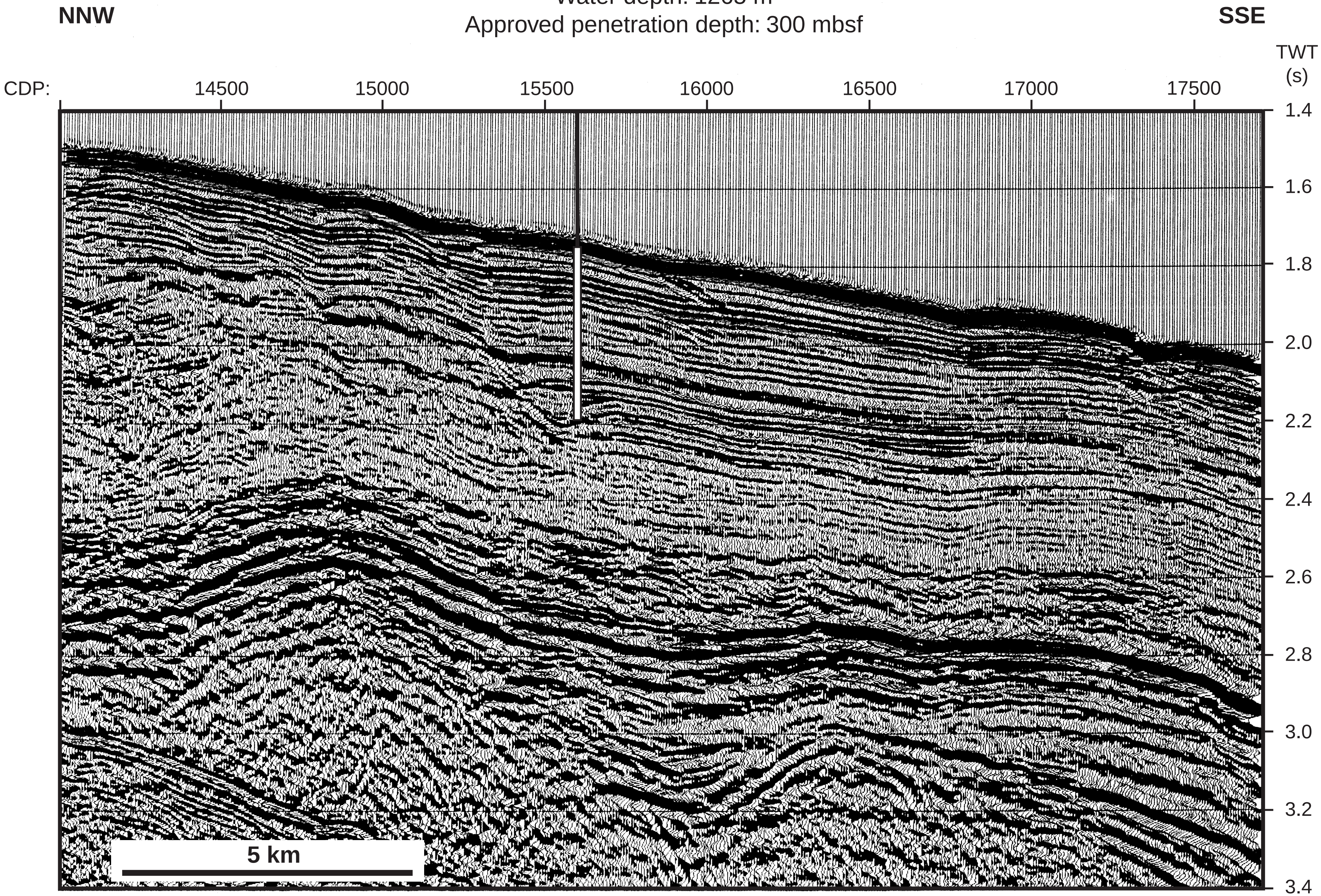

Site: SCS-3C

Priority: 1
Position: 19° 59.76'N, 116°0.90'E
Water Depth: 1265 m
Sediment Thickness: 810 m
Approved Maximum Penetration: 300 m
Seismic Coverage: Intersection of SO-95 Profile 5 and SO-72A Profile 18

Objectives:

1. To recover a continuous sequence of hemipelagic sediments to reconstruct the late Miocene (?) to Pleistocene paleomonsoon history.

2. To determine the characteristics and variability of upper slope sediments bathed in intermediate waters, possibly with low oxygen content.

3. To provide the shallow end-member (1265 m) for the Plio-Pleistocene depth transect to examine the vertical gradients of water mass properties and carbonate preservation.

Drilling Program: Single APC to refusal, XCB to 300 mbsf

Logging and Downhole Operations: None

Nature of Rock Anticipated: Hemipelagic mud and silt

Proposed Site SCS-4

Line SO95-5, CDP 1025 (17:55)

Water depth: 2093 m

Approved penetration depth: 500 mbsf

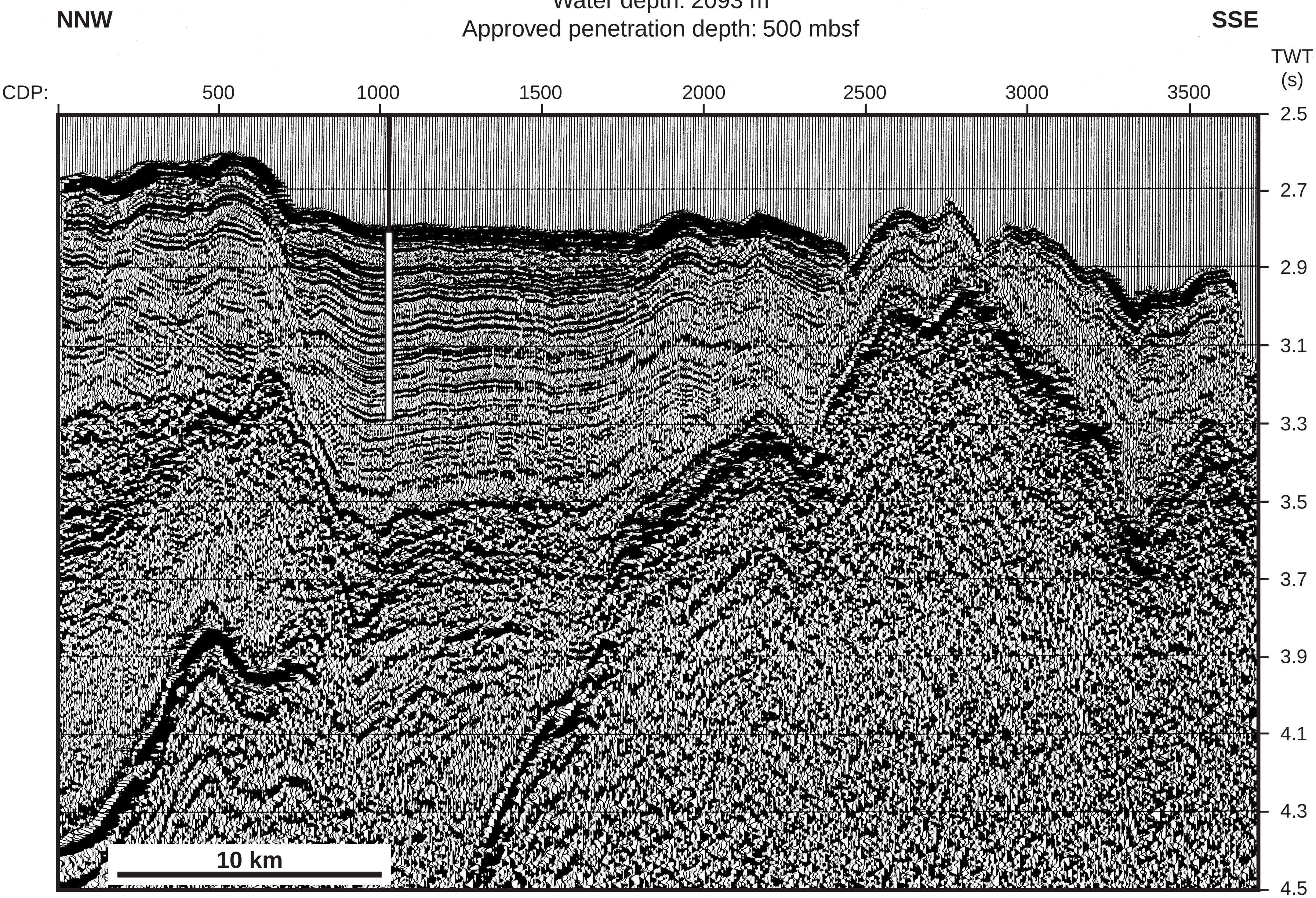

Site: SCS-4

Priority: 1
Position: 19°27.24'N, 116°15.84'E
Water Depth: 2093 m
Sediment Thickness: 1400 m
Approved Maximum Penetration: 520 m
Seismic Coverage: Intersection of SO-95 Profile 5

Objectives:

1. To recover a continuous sequence of hemipelagic sediments to reconstruct the middle Miocene to Pliocene paleomonsoon history.

2. To identify if monsoonal indices intensify or weaken during the middle to late Miocene as a test of monsoon evolution models.

3. To establish if Miocene-Pliocene pattern of accumulation rates are consistent with models of HTC uplift, monsoon intensification, and sea-level changes.

Drilling Program: Triple APC to refusal, XCB (possibly double XCB) to 520 mbsf

Logging and Downhole Operations: Triple-combo, GHMT, and sonic-FMS

Nature of Rock Anticipated: Hemipelagic mud and silt

Proposed Site SCS-5C

Line SO95-5, CDP 7500 (1:57)

Water depth: 3232 m

Approved penetration depth: 700 mbsf

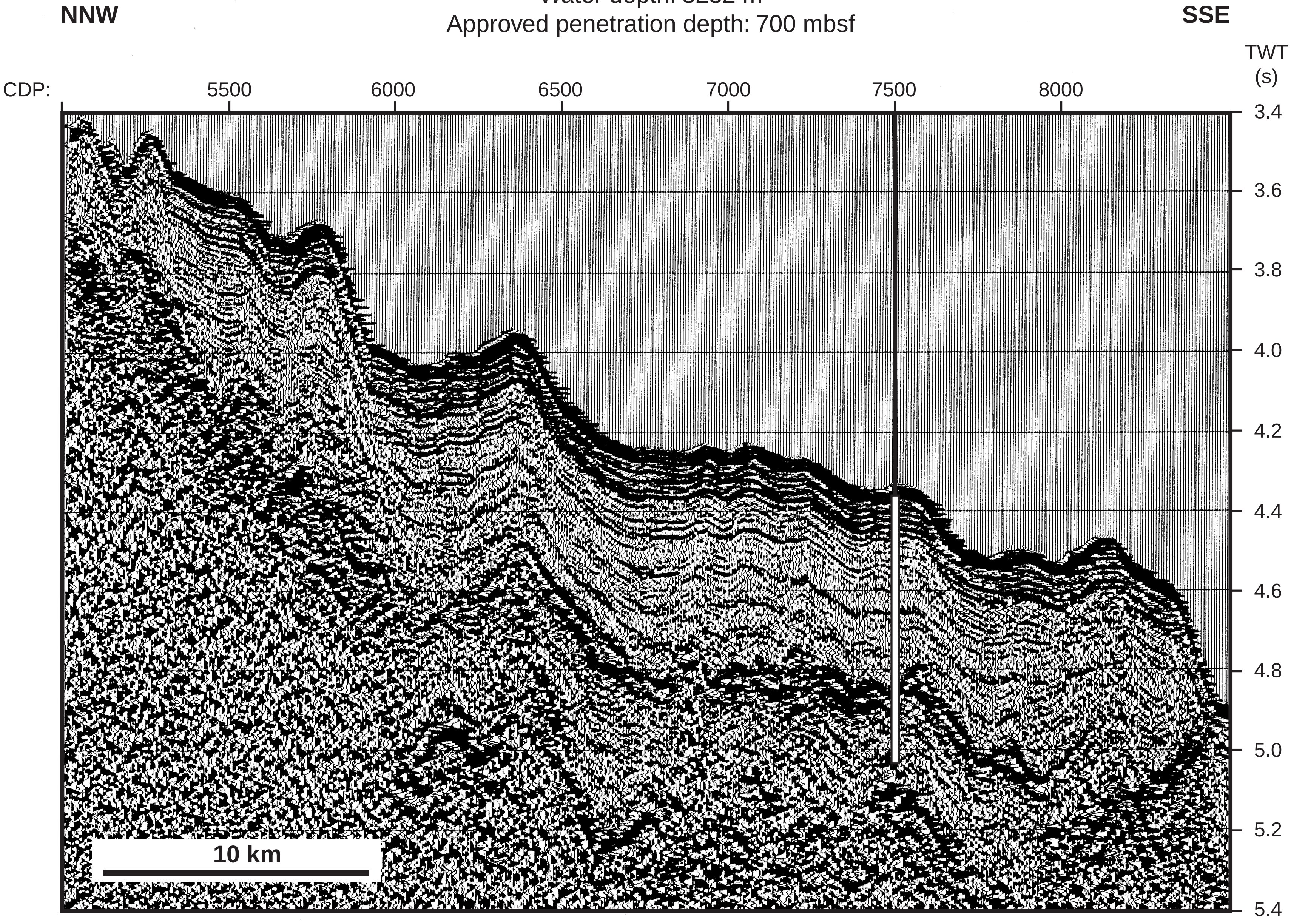

Site: SCS-5C

Priority: 1
Position: 18°49.73'N, 116°32.93'E
Water Depth: 3232 m
Sediment Thickness: 750 m
Approved Maximum Penetration: 700 m
Seismic Coverage: SO-95 Profile 5 near intersection with Profile 20

Objectives:

1. To recover a continuous sequence of hemipelagic sediments to reconstruct the paleoclimate history from Oligocene to Miocene.

2. To identify the onset of monsoonal variability in the SCS and to establish its evolution in the Oligo-Miocene interval.

3. To establish if Oligo-Miocene pattern of accumulation rates are consistent with models of HTC uplift, monsoon intensification, and sea-level changes.

Drilling Program: Triple APC to refusal, XCB (possibly double XCB) to 450 m, RCB to 700 m

Logging and Downhole Operations: Triple-combo, GHMT, and sonic-FMS

Nature of Rock Anticipated: Hemipelagic mud and silt

Proposed Site SCS-5D

Line SO95-20, CDP 1925 (15:49)
Water depth: 2682 m
Approved penetration depth: 770 mbsf

NE SW

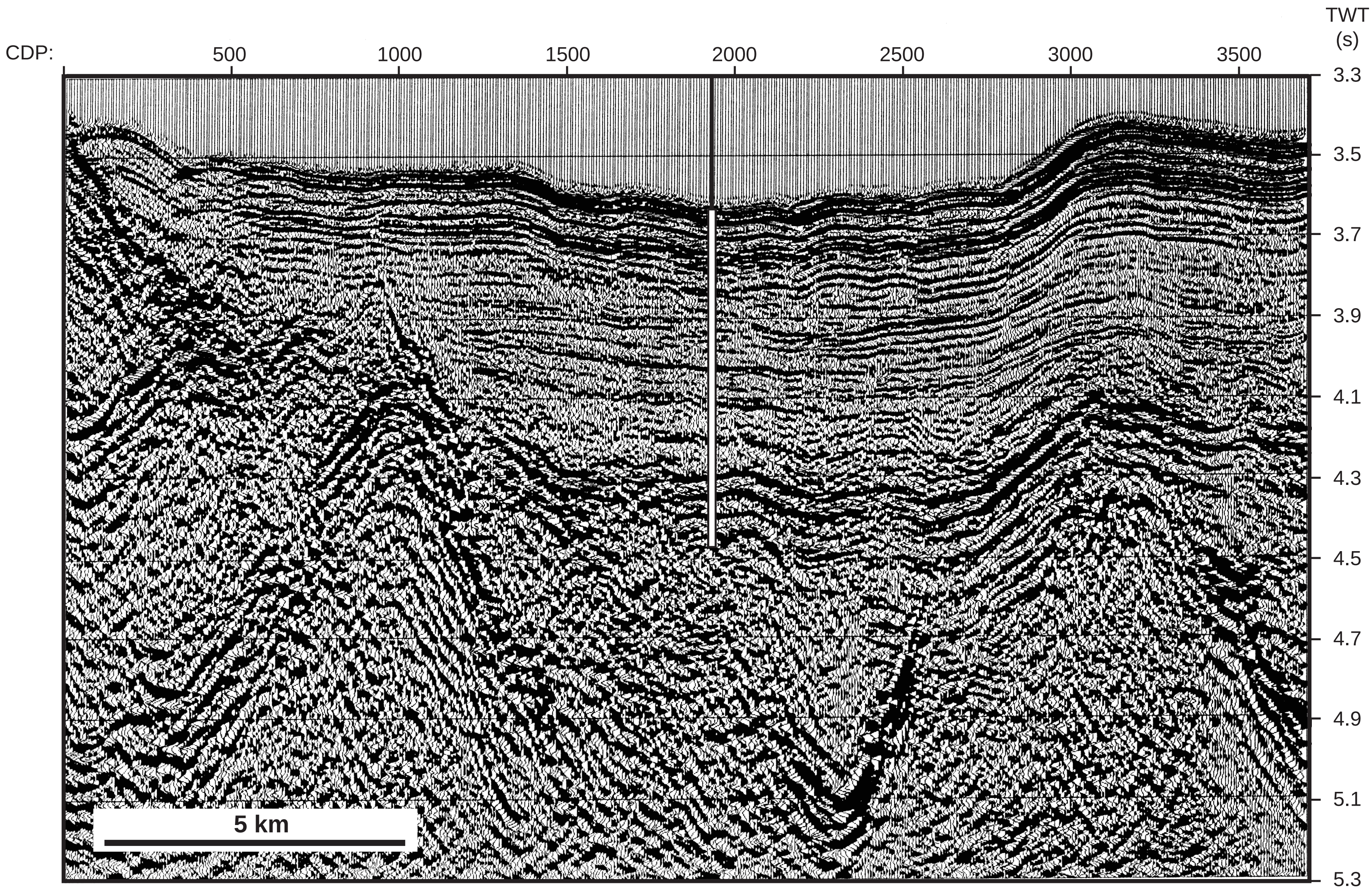

Site: SCS-5D

Priority: 1
Position: 19°20.94'N, 116°51.66'E
Water Depth: 2682 m
Sediment Thickness: 1160 m
Approved Maximum Penetration: 700 m
Seismic Coverage: SO-95 Profile 20

Objectives:

1. To recover a continuous sequence of hemipelagic sediments to reconstruct the paleoclimate history from Oligocene to Miocene.

2. To identify the onset of monsoonal variability in the SCS and to establish its evolution in the Oligo-Miocene interval.

3. To establish if Oligocene-Miocene pattern of accumulation rates are consistent with models of HTC uplift, monsoon intensification, and sea-level changes.

Drilling Program: Triple APC to refusal, XCB (possibly double XCB) to 450 m, RCB to 700 m

Logging and Downhole Operations: Triple-combo, GHMT, and sonic-FMS

Nature of Rock Anticipated: Hemipelagic mud and silt

Proposed Site SCS-5E

Line SO95-20, CDP 8430 (21:27)

Water depth: 3143 m

Approved penetration depth: 710 mbsf

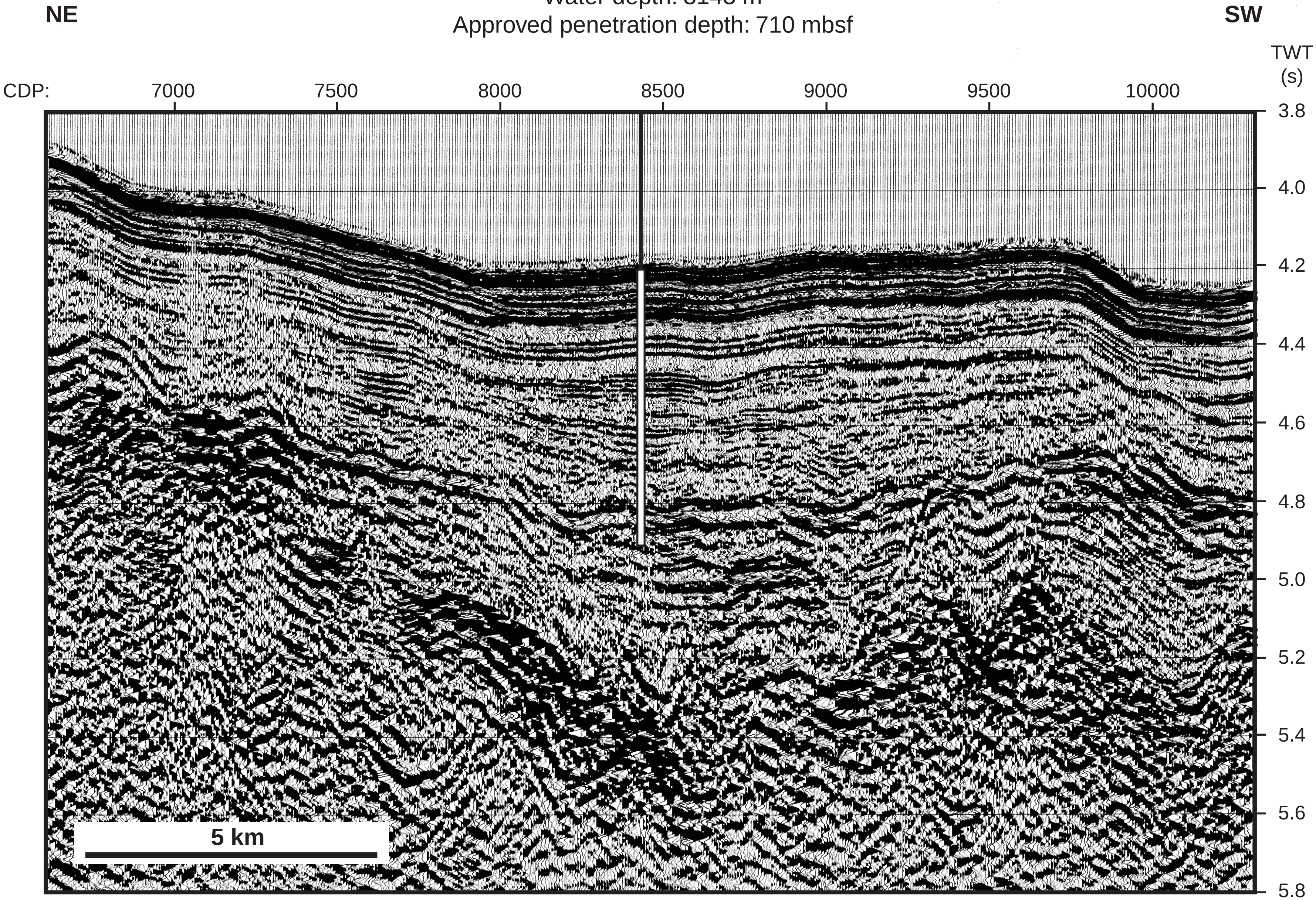

Site: SCS-5E

Priority: 1
Position: 19°0.36'N, 116°35.88'E
Water Depth: 3143 m
Sediment Thickness: 1160 m
Approved Maximum Penetration: 770 m
Seismic Coverage: SO-95 Profile 20

Objectives:

1. To recover a continuous sequence of hemipelagic sediments to reconstruct the paleoclimate history from Oligocene to Miocene.

2. To identify the onset of monsoonal variability in the SCS and to establish its evolution in the Oligocene-Miocene interval.

3. To establish if Oligocene-Miocene pattern of accumulation rates are consistent with models of HTC uplift, monsoon intensification, and sea-level changes.

Drilling Program: Triple APC to refusal, XCB (possibly double XCB) to 450 m, RCB to 770 m

Logging and Downhole Operations: Triple-combo, GHMT, and sonic-FMS

Nature of Rock Anticipated: Hemipelagic mud and silt

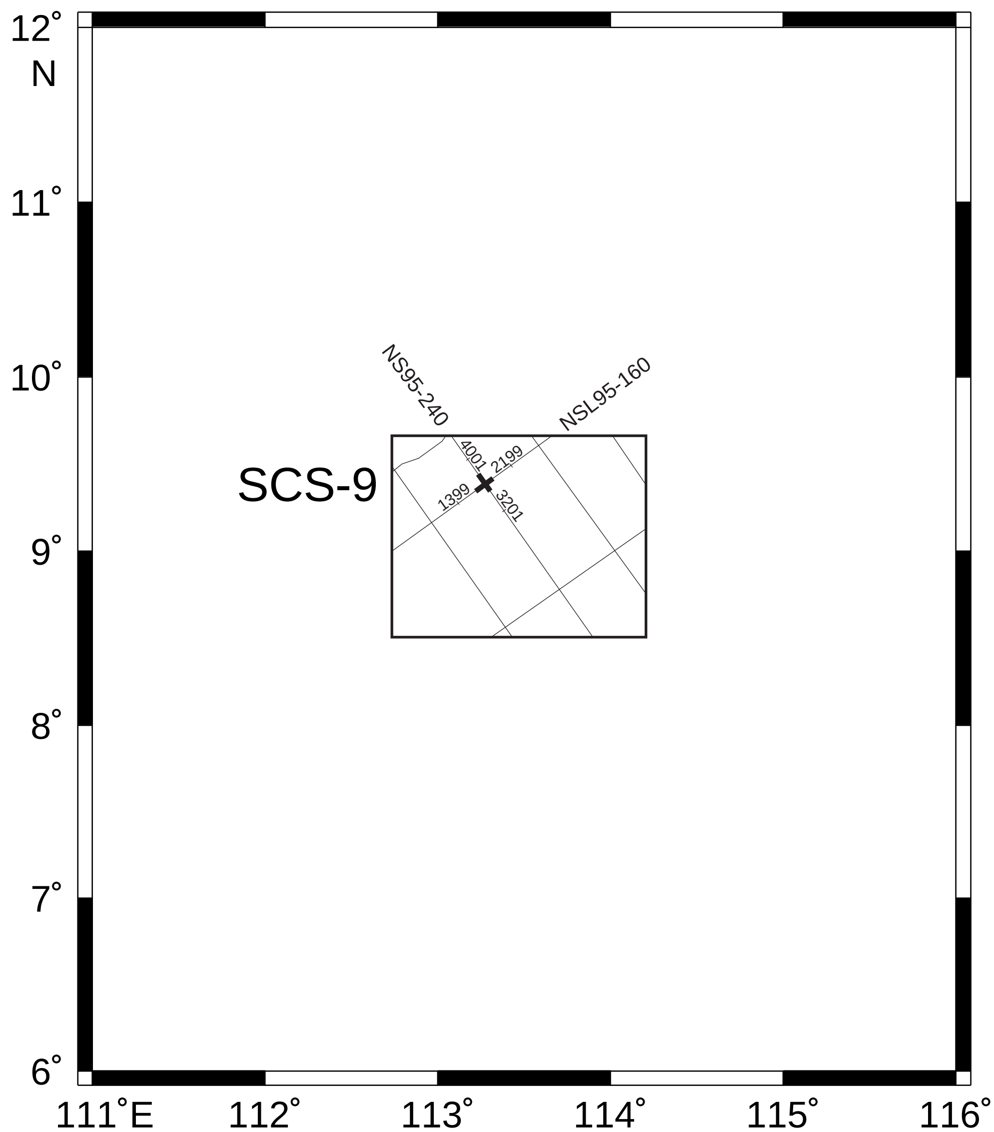

Parts of seismic survey lines and proposed site location in the southern SCS drilling area. Larger frame corresponds to the area shown in Figure 2 (overview) and Figure 10 (bathymetry). Inset with track lines corresponds to the navigation data received. Cross in bold lines corresponds to the seismic sections shown in the site description.

Site: SCS-9

Priority: 1
Position: 09°21.72'N, 113°17.10'E
Water Depth: 2830 m
Sediment Thickness: 1010 m
Approved Maximum Penetration: 400 m
Seismic Coverage: Intersection of lines NS95-240 and NSL95-160

Objectives:

1. To recover a continuous sediment record to reconstruct the paleoclimate history in the tropical SCS during the late Neogene.

2. To determine variations in the supply of terrigenous sediment from the Mekong and southern sources.

3. To establish the record of SST variability in the SCS as a measure of the Western Pacific Warm Pool and for comparison to the seasonal SST patterns of the northern SCS.

Drilling Program: Triple APC to refusal, XCB to 400 mbsf

Logging and Downhole Operations: Triple-combo, GHMT, and sonic FMS

Nature of Rock Anticipated: Hemipelagic mud, silt, and other clastic sediments and rocks

Proposed Site SCS-9

Line NS95-240, CDP 3617

Water depth: 2830 m

Approved penetration depth: 400 mbsf

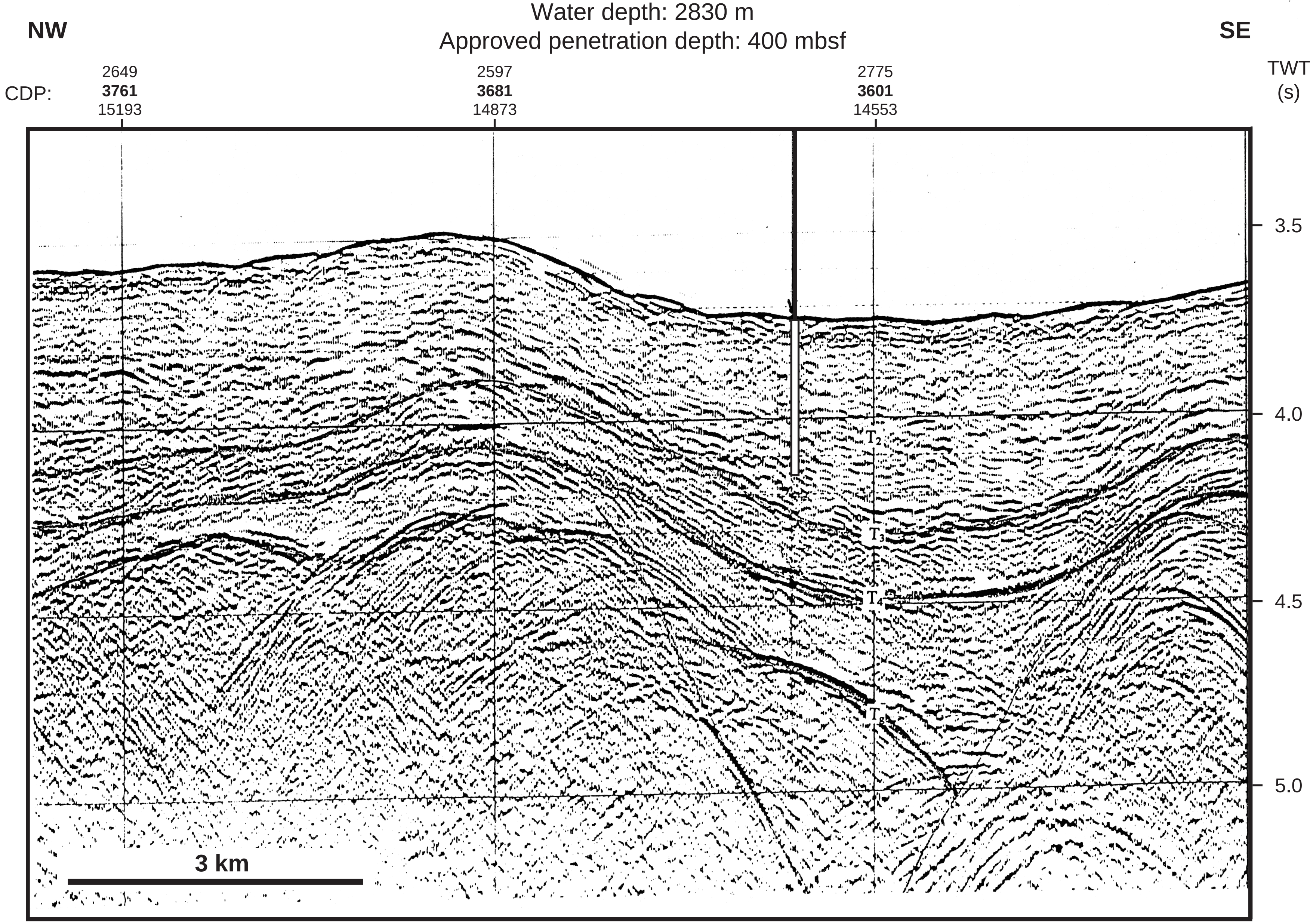

Proposed Site SCS-9
Line NSL95-160, CDP 1812
Water depth: 2830 m
Approved penetration depth: 400 mbsf

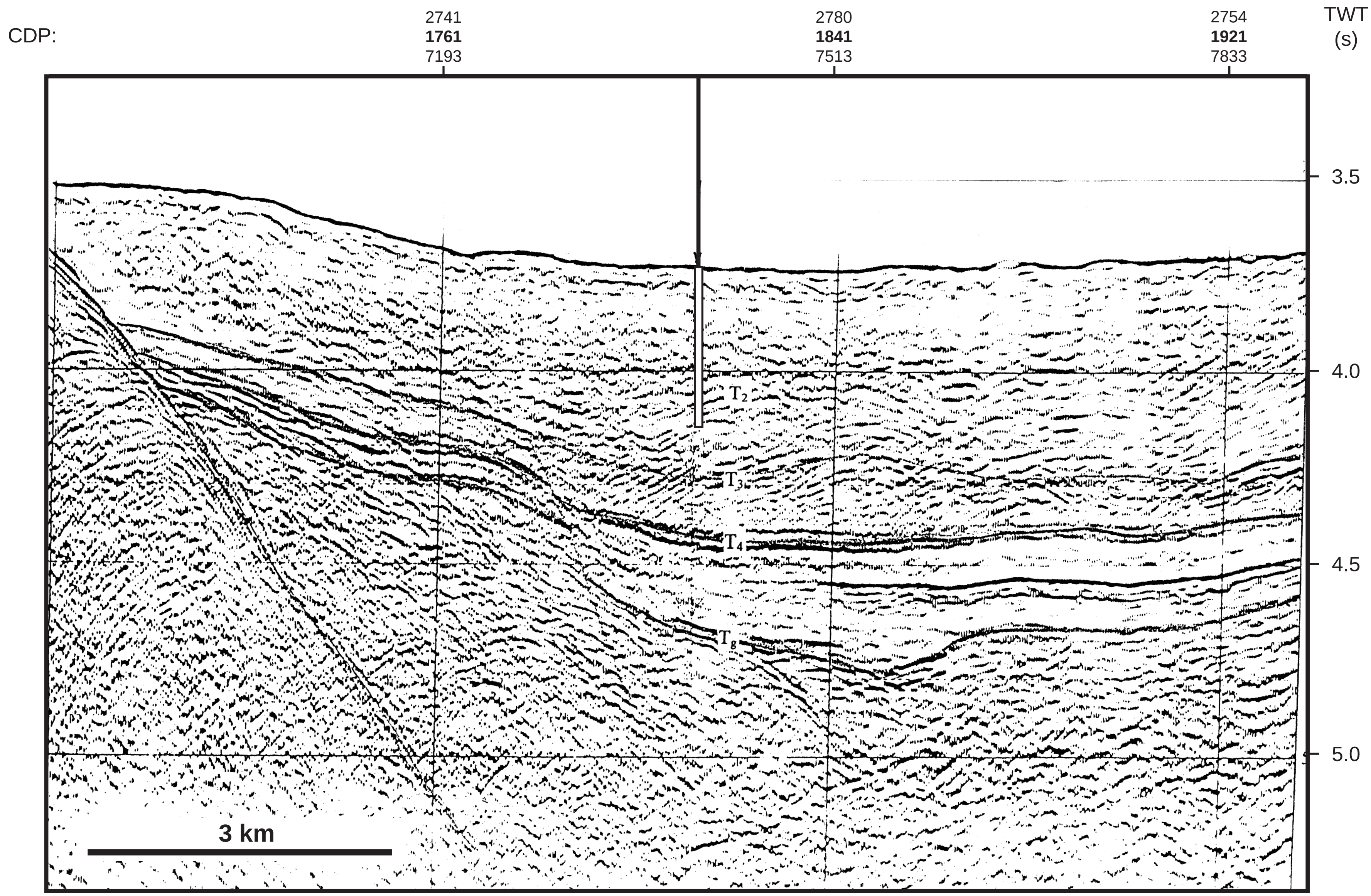

Scientific Participants

Co-Chief
Warren L. Prell
Department of Geological Sciences
Brown University
Box 1846
Providence, RI 02912
U.S.A.
Internet: warren_prell@brown.edu
Work: (401) 863-3221
Fax: (401) 863-2058

Co-Chief
Pinxian Wang
Department of Marine Geology and Geophysics
Tongji University
Shanghai 200092
People's Republic of China
Internet: pxwang@online.sh.cn
Work: (86) 21-6598-3207
Fax: (86) 21-6513-8808

Staff Scientist
Peter Blum
Ocean Drilling Program
Texas A&M University
1000 Discovery Drive
College Station, TX 77845-9547
U.S.A.
Internet: peter_blum@odp.tamu.edu
Work: (409) 845-9299
Fax: (409) 845-0876

Inorganic Geochemist
Christophe J. G. Colin
Laboratoire de Geochemie des Roches
Sedimentaires
Université de Paris-Sud XI
BAT. 504
Orsay Cedex 91405
France
Internet: colin@geol.u-psud.fr
Work: (33) 1-69-15-67-45
Fax: (33) 1-69-15-48-82

Inorganic Geochemist
Katherine McIntyre
Marine Sciences Institute
University of California, Santa Barbara
Santa Barbara, CA 93106
U.S.A.
Internet: mcintyre@lifesci.ucsb.edu
Work: (805) 893-7061
Fax: (805) 893-8062

Organic Geochemist
Matthew J. Higginson
School of Chemistry
University of Bristol
Cantock's Close
Bristol BS8 1TS
United Kingdom
Internet: matthew.higginson@bristol.ac.uk
Work: (44) 117-928-9000, ext 4430
Fax: (44) 117-929-3746

Organic Geochemist
Joel S. Leventhal
Private Consultant: U.S.A.
Diversified Geochemistry
8944 W. Warren Dr.
Lakewood, CO 80227
U.S.A.
Internet: hoflev@aol.com
Work: (303) 988-7269

JOIDES Logging Scientist
Jian Lin
Department of Geology and Geophysics
Woods Hole Oceanographic Institution
Woods Hole, MA 02543
U.S.A.
Internet: jlin@whoi.edu
Work: (508) 289-2576
Fax: (508) 457-2187

Paleomagnetist
Carlo E. Laj
Laboratoire des Sciences du Climat et de l'Environnement (LSCE)
CNRS
Bat. 12
Avenue de la Terrasse
Gif-sur-Yvette Cedex 91198
France
Internet: laj@lsce.cnrs-gif.fr
Work: (33) 1-69-82-35-38
Fax: (33) 1-69-82-35-68

Paleomagnetist
Peter A. Solheid
Institute for Rock Magnetism
University of Minnesota, Minneapolis
287 Shepherd Laboratories
Minneapolis, MN 55455-0128
U.S.A.
Internet: peat@umn.edu
Work: (612) 624-5274
Fax: (612) 625-7502

Paleontologist (Foraminifer)
Zhimin Jian
Department of Marine Geology and Geophysics
Tongji University
Siping Road 1239
Shanghai 200092
People's Republic of China
Internet: zjiank@online.sh.cn
Work: (86) 21-6598-3207
Fax: (86) 21-6513-8808

Paleontologist (Foraminifer)
Stephen A. Nathan
Department of Geosciences
University of Massachusetts
Morrill Science Center
Amherst, MA 01003
U.S.A.
Internet: snathan@geo.umass.edu
Work: (413) 545-2016
Fax: (413) 545-4884

Paleontologist (Nannofossil)
Jih-Ping Shyu
Institute of Oceanography
National Taiwan University
P.O. Box 23-13
Taipei 10617
Taiwan
Internet: jpshyu@iodec1.oc.ntu.edu.tw
Work: (886) 2-391-4442
Fax: (886) 2-391-4442

Paleontologist (Nannofossil)
Xin Su
Department of Geology
China University of Geosciences
Xueyuan Road 29
Beijing 100083
People's Republic of China
Internet: xsu@sky.cugb.edu.cn
Work: (86)10-62312244-2261
Fax: (86)10-62937940

Physical Properties Specialist
Christian J. Bühring
Geologisch-Paläontologisches Institut
Christian-Albrechts-Universität zu Kiel
Olshausenstrasse 40
Kiel 24118
Federal Republic of Germany
Internet: cb@zaphod.gpi.uni-kiel.de
Work: (49) 431-880-2966
Fax: (49) 431-880-4367

Physical Properties Specialist
Min-Pen Chen
Institute of Oceanography
National Taiwan University
P.O. Box 23-13
Taipei 10617
Taiwan
Internet: minpen@ccms.ntu.edu.tw
Work: (886) 2-2391-4442
Fax: (886) 2-2364-4049

Sedimentologist
Eve M. Arnold
Geologi och Geokemi
Stockholms Universitet
Stockholm 106 91
Sweden
Internet: emarnold@geo.su.se
Work: (46) 867-47598
Fax: (46) 867-47897

Sedimentologist
Peter D. Clift
Department of Geology and Geophysics
Woods Hole Oceanographic Institution
MS#22
Woods Hole, MA 02543
U.S.A.
Internet: pclift@whoi.edu
Work: (508) 289-3437
Fax: (508) 457-2187

Sedimentologist
Wolfgang Kuhnt
Geologisch-Paläontologisches Institut
Christian-Albrechts-Universität zu Kiel
Olshausenstraße 40
Kiel 24118
Federal Republic of Germany
Internet: wk@gpi.uni-kiel.de
Work: (49) 431-880-2924
Fax: (49) 431-880-4376

Sedimentologist
Anchun Li
Institute of Oceanology
Chinese Academy of Sciences
7 Nanhai Road
Qingdao, Shandong Province 266071
People's Republic of China
Internet: acli@ms.qdio.ac.cn
Work: (86) 532-287-9062, ext 2214
Fax: (86) 532-287-0882

Sedimentologist
Federica Tamburini
Insitute de Géologie
Université de Neuchâtel
Rue Emile Argand, 11
Neuchâtel 2007
Switzerland
Internet: federica.tamburini@geol.unine.ch
Work: (41) 32-718-26-20
Fax: (41) 32-718-26-01

Sedimentologist
Alain Trentesaux
Laboratoire de Sédimentologie et
Géodynamique
Université de Lille I
SN5
Villeneuve d'Ascq Cedex 59655
France
Internet: alain.trentesaux@univ-lille1.fr
Work: (33) 3-20-43-49-10
Fax: (33) 3-20-43-49-15

Sedimentologist
Luejiang Wang
Graduate School of Environmental Earth
Science
Hokkaido University
Nishi 5 Kita 10 Kita Ku
Sapporo 060-0810
Japan
Internet: ljwang@ees.hokudai.ac.jp
Work: (81) 11-706-5303
Fax: (81) 11-736-3290

Stratigraphic Correlator
Steven C. Clemens
Department of Geological Sciences
Brown University
Box 1846
Providence, RI 02912-1846
U.S.A.
Internet: steven_clemens@brown.edu
Work: (401) 863-1964
Fax: (401) 863-2058

Stratigraphic Correlator
John W. Farrell
Joint Oceanographic Institutions Inc.
1755 Massachusetts Ave. NW
Suite 800
Washington, DC 20036-2102
U.S.A.
Internet: jfarrell@brook.edu
Work: (202) 232-3900
Fax: (202) 232-8203

LDEO Logging Scientist
Christine Lauer
Laboratoire de Géochimie Isotopique
Université Montpellier II
ISTEEM
Case 066 - Place Eugene Bataillon
Montpellier Cedex 05 34095
France
Internet: christine.lauer-leredde@dstu.univ-montp2.fr
Work: (33) 4-42-97-11-33
Fax: (33) 4-42-97-11-21

LDEO Logging Trainee
Qingmou Li
Institute of Geophysics
Chinese Academy of Sciences
P.O. Box 9701
A-11 Datun Road
Beijing 100101
People's Repubilc of China
Internet: qmlee@c-geos15.c-geos.ac.cn
Work:
Fax: (86) 10-6487-1995

Schlumberger Engineer
Robert Laronga
Schlumberger Offshore Services
369 Tristar Drive
Webster, TX 77598
U.S.A.
Internet: laronga@webster.wireline.slb.com
Work: (281) 480-2000
Fax: (281) 480-9550

Operations Manager
Ron Grout
Ocean Drilling Program
Texas A&M University
1000 Discovery Drive
College Station, TX 77845-9547
U.S.A.
Internet: ron_grout@odp.tamu.edu
Work: (409) 845-2144
Fax: (409) 845-2308

Laboratory Officer
Kuro Kuroki
Ocean Drilling Program
Texas A&M University
1000 Discovery Drive
College Station, TX 77845-9547
U.S.A.
Internet: kuro_kuroki@odp.tamu.edu
Work: (409) 845-8482
Fax: (409) 845-0876

Marine Lab Specialist: Yeoperson
Michiko Hitchcox
Ocean Drilling Program
Texas A&M University
1000 Discovery Drive
College Station, TX 77845-9547
U.S.A.
Internet: michiko_hitchcox@odp.tamu.edu
Work: (409) 845-2483
Fax: (409) 845-0876

Marine Lab Specialist: Chemistry
Dennis Graham
Ocean Drilling Program
Texas A&M University
1000 Discovery Drive
College Station, TX 77845-9547
U.S.A.
Internet: dennis_graham@odp.tamu.edu
Work: (409) 845-8482
Fax: (409) 845-0876

Marine Lab Specialist: Chemistry
Chieh Peng
Ocean Drilling Program
Texas A&M University
1000 Discovery Drive
College Station, TX 77845-9547
U.S.A.
Internet: chieh_peng@odp.tamu.edu
Work: (409) 845-2480
Fax: (409) 845-0876

Marine Lab Specialist: Core
Maniko Kamei
Ocean Drilling Program
Texas A&M University
1000 Discovery Drive
College Station, TX 77845-9547
U.S.A.
Internet: maniko_kamei@odp.tamu.edu

Marine Lab Specialist: Curator
Gerald Bode
Scripps Institution of Oceanography
University of California, San Diego
Ocean Drilling Program
West Coast Repository
La Jolla, CA 92093-0231
U.S.A.
Internet: gerald_bode@odp.tamu.edu
Work: (619) 534-1657

Marine Lab Specialist: Assistant Curator
Peter Esmay
Lamont-Doherty Earth Observatory
Columbia University
ODP East Coast Repository
Route 9W
Palisades, NY 10964
U.S.A.
Internet: peter.esmay@odp.tamu.edu
Work: (914) 365-8446
Fax: (914) 365-8178

Marine Lab Specialist: Downhole Tools,
Marine Lab Specialist: Thin Sections
Gus Gustafson
Ocean Drilling Program
Texas A&M University
1000 Discovery Drive
College Station, TX 77845-9547
U.S.A.
Internet: ted_gustafson@odp.tamu.edu
Work: (409) 845-8482
Fax: (409) 845-0876

Marine Lab Specialist: Paleomagnetics
Charles A. Endris
Ocean Drilling Program
Texas A&M University
1000 Discovery Drive
College Station, TX 77845
U.S.A.
Work: (409) 845-5135
Fax: (409) 845-0876

Marine Lab Specialist: Photographer
Tim Fulton
Ocean Drilling Program
Texas A&M University
1000 Discovery Drive
College Station, TX 77845-9547
U.S.A
Internet: tim_fulton@odp.tamu.edu
Work: (409) 845-1183
Fax: (409) 845-4857

Marine Lab Specialist: Physical Properties
Anastasia Ledwon
Ocean Drilling Program
Texas A&M University
1000 Discovery Drive
College Station, TX 77845-9547
U.S.A.
Internet: anastasia_ledwon@odp.tamu.edu
Work: (409) 845-9186
Fax: (409) 845-0876

Marine Lab Specialist: Underway Geophysics
Don Sims
Ocean Drilling Program
Texas A&M University
1000 Discovery Drive
College Station, TX 77845-9547
U.S.A.
Internet: don_sims@odp.tamu.edu
Work: (409) 845-2481
Fax: (409) 845-0876

Marine Lab Specialist: X-Ray
Robert Olivas
Ocean Drilling Program
Texas A&M University
1000 Discovery Drive
College Station, TX 77845-9547
U.S.A.
Internet: bob_olivas@odp.tamu.edu
Work: (409) 845-2481
Fax: (409) 845-0876

Marine Lab Specialist: Marine Logistics Coordinator
Larry Obee
Ocean Drilling Program
Texas A&M University
1000 Discovery Drive
College Station, TX 77845-9547
U.S.A.
Internet: larry_obee@odp.tamu.edu
Work: (409) 862-8717
Fax: (409) 845-2380

Marine Electronics Specialist
Randy W. Gjesvold
Ocean Drilling Program
Texas A&M University
1000 Discovery Drive
College Station , TX 77845-9547
U.S.A.
Internet: randy_gjesvold@odp.tamu.edu

Marine Electronics Specialist
Larry St. John
Ocean Drilling Program
Texas A&M University
1000 Discovery Drive
College Station, TX 77845-9547
U.S.A.
Internet: larry_st.john@odp.tamu.edu
Work: (409) 845-2454
Fax: (409) 845-2308

Marine Computer Specialist
Mike Hodge
Ocean Drilling Program
Texas A&M University
1000 Discovery Drive
College Station, TX 77845-9547
U.S.A.
Internet: mike_hodge@odp.tamu.edu
Work: (409) 862-4845
Fax: (409) 845-4857

Marine Computer Specialist
David Kotz
Ocean Drilling Program
Texas A&M University
1000 Discovery Drive
College Station, TX 77845-9547
U.S.A.
Internet: david_kotz@odp.tamu.edu
Work: (409) 862-4848
Fax: (409) 845-4857